The histone acetyltransferase CBP participates in regulating the DNA damage response through ATM after double-strand breaks

RAMADAN, Wafaa S., AHMED, Samrein <http://orcid.org/0000-0001-9773-645X>, TALAAT, Iman M., LOZON, Lama, MOUFFAK, Soraya, GEMOLL, Timo, MANSOUR, Wael Y. and EL-AWADY, Raafat

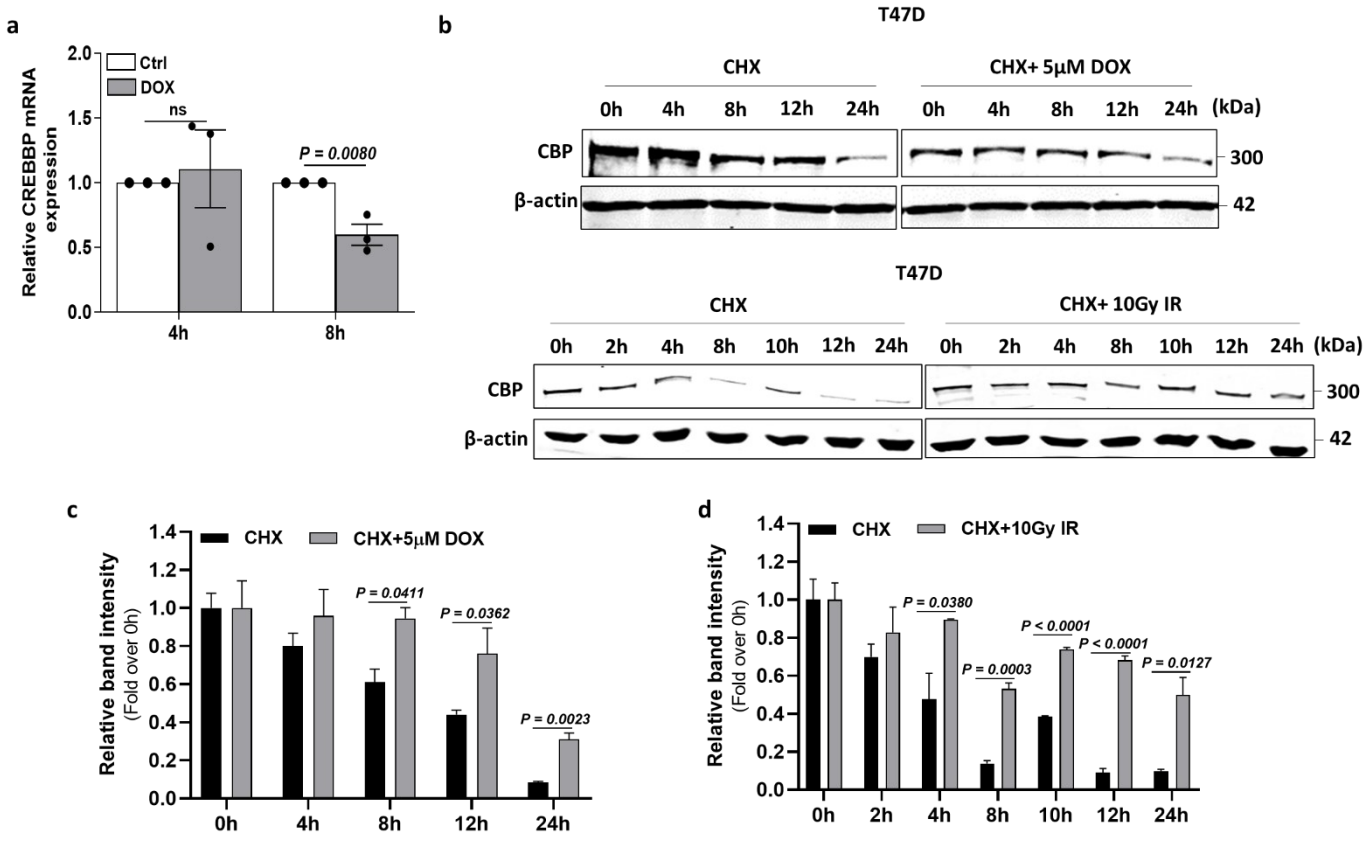

Fig. S1 CBP protein level is stabilized under DNA damage induction. a Real-Time PCR was used to measure the relative mRNA levels of the *CREBBP* gene, normalized to *GAPDH,* in T47D cells incubated with 5μM of Doxorubicin (DOX) for the indicated time points. **b** CBP protein stability was analyzed by a cycloheximide-chase assay at the indicated time points. Immunoblotting analysis was performed on T47D cells incubated with cycloheximide (CHX) alone and in combination with DOX. The T47D cells were irradiated with 10 Gy in the presence of CHX. **c**, **d** Graphs show the quantification of CBP band intensities, normalized to β-actin, and presented as fold change relative to the 0h time point. Data are represented as mean ± SEM, n=2. $P < 0.05$ is considered significant, Mann–Whitney U test.

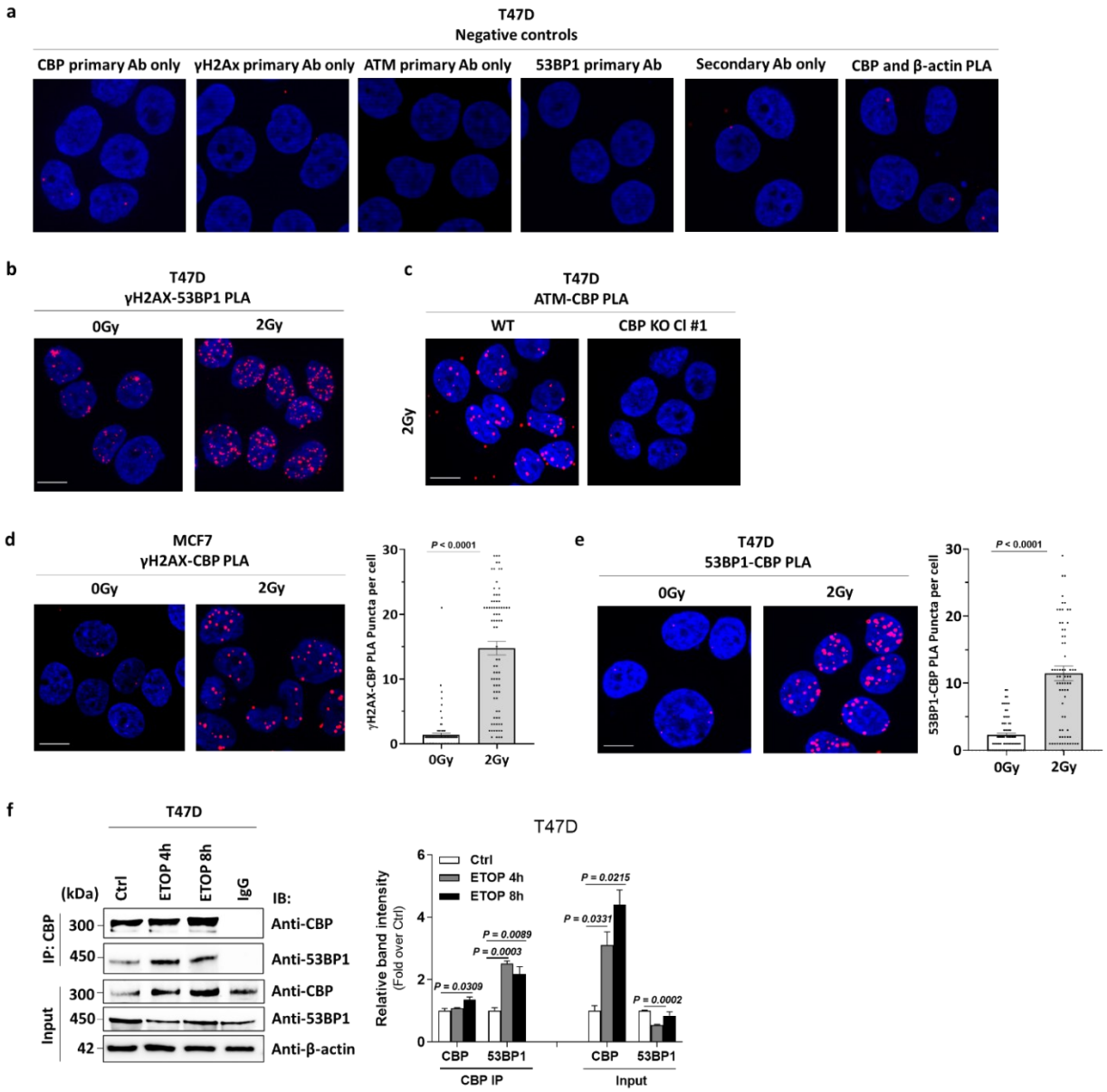

Figure S2. Analysis of CBP interactions with DNA damage response proteins. a Negative controls for Proximity ligation assay (PLA). **b** Positive controls for PLA. Scale bar, 100μm. **c** PLA for ATM and CBP in T47D wild-type (WT) and CBP knockout (KO) cells following ionizing radiation (IR). Scale bar, 100μm. **d**, **e** Left panel: PLA detecting CBP and γH2AX colocalization (red) in MCF7 cells (**d**) and 53BP1 and CBP colocalization in T47D cells (**e**) at 5mins after 2Gy IR. DAPI (blue) stains the nuclear regions. Scale bar, 100μm. Right panel: Quantification of PLA signals from 100 cells. **f** Left panel: Immunoprecipitation (IP) of CBP from T47D cells treated with Etoposide (ETOP) for 4 and 8h. Immunocomplexes were analyzed by immunoblotting with anti-53BP1. Right panel: Band quantification of CBP and 53BP1 in immunoprecipitated and input samples. Data are represented as mean ± SEM, n=2. $P < 0.05$ is considered significant, Mann–Whitney U test.

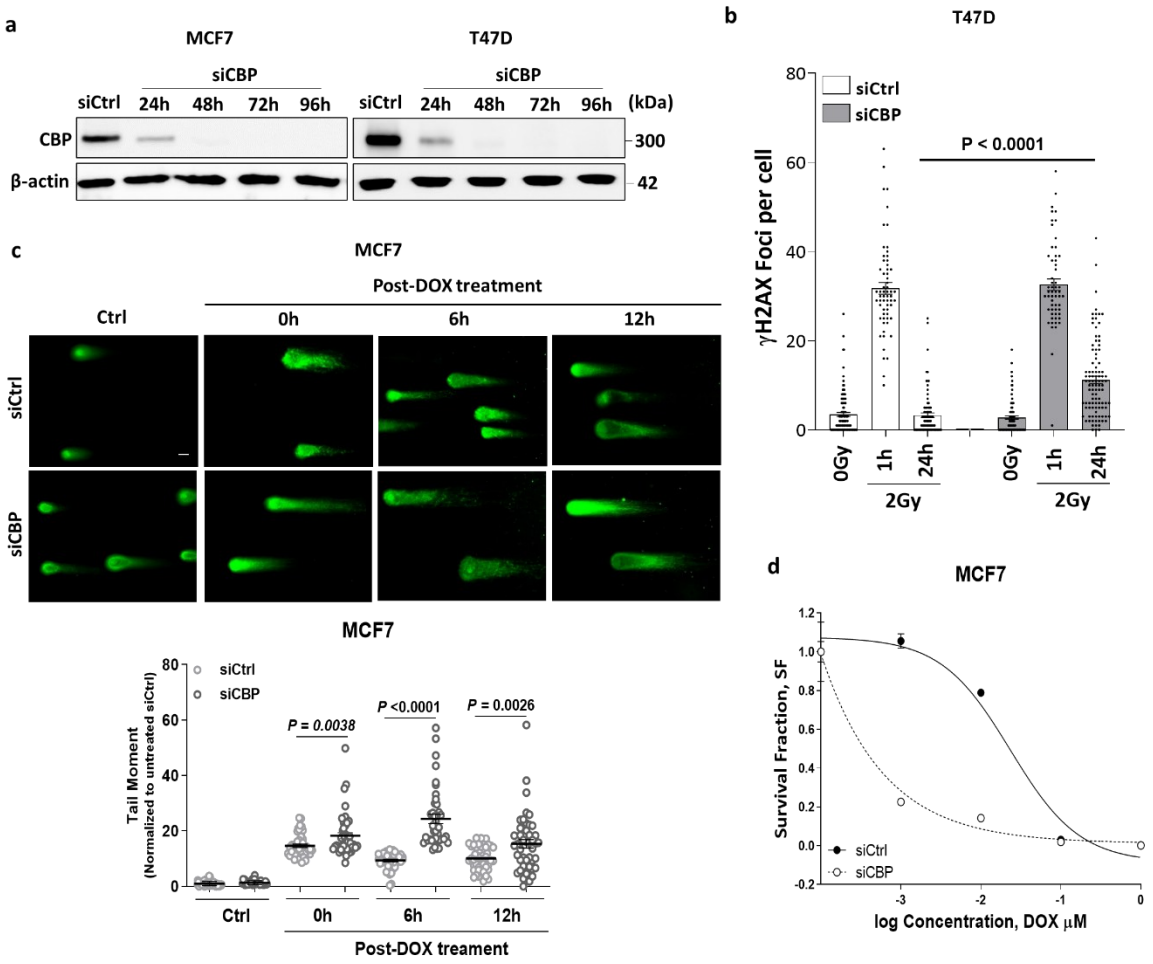

Fig. S3 DNA repair efficiency after DNA damage induction in CBP-depleted T47D and MCF7 cells. a Validation of siRNA-mediated depletion of CBP protein in MCF7 and T47D cells. **b** Quantification of γH2Ax foci in T47D cells at 1 and 24h post-2Gy ionizing radiation (IR). The total number of γH2Ax foci per cell was counted from 100 cells**. c** Upper panel: Images of neutral comet assay at 0, 6 and 12h after Doxorubicin (DOX) removal in MCF7 cells transfected with control or CBP siRNA. Scale bar, 50μm. Lower panel: Quantification of the neutral comet assay via tail moment in MCF7 cells from 50 cells. **d** Colony formation assay of MCF7 cells transfected with the indicated siRNA and incubated with different concentrations of DOX. Data are represented as mean ± SEM, n=3. $P < 0.05$ is considered significant, Mann–Whitney U test.

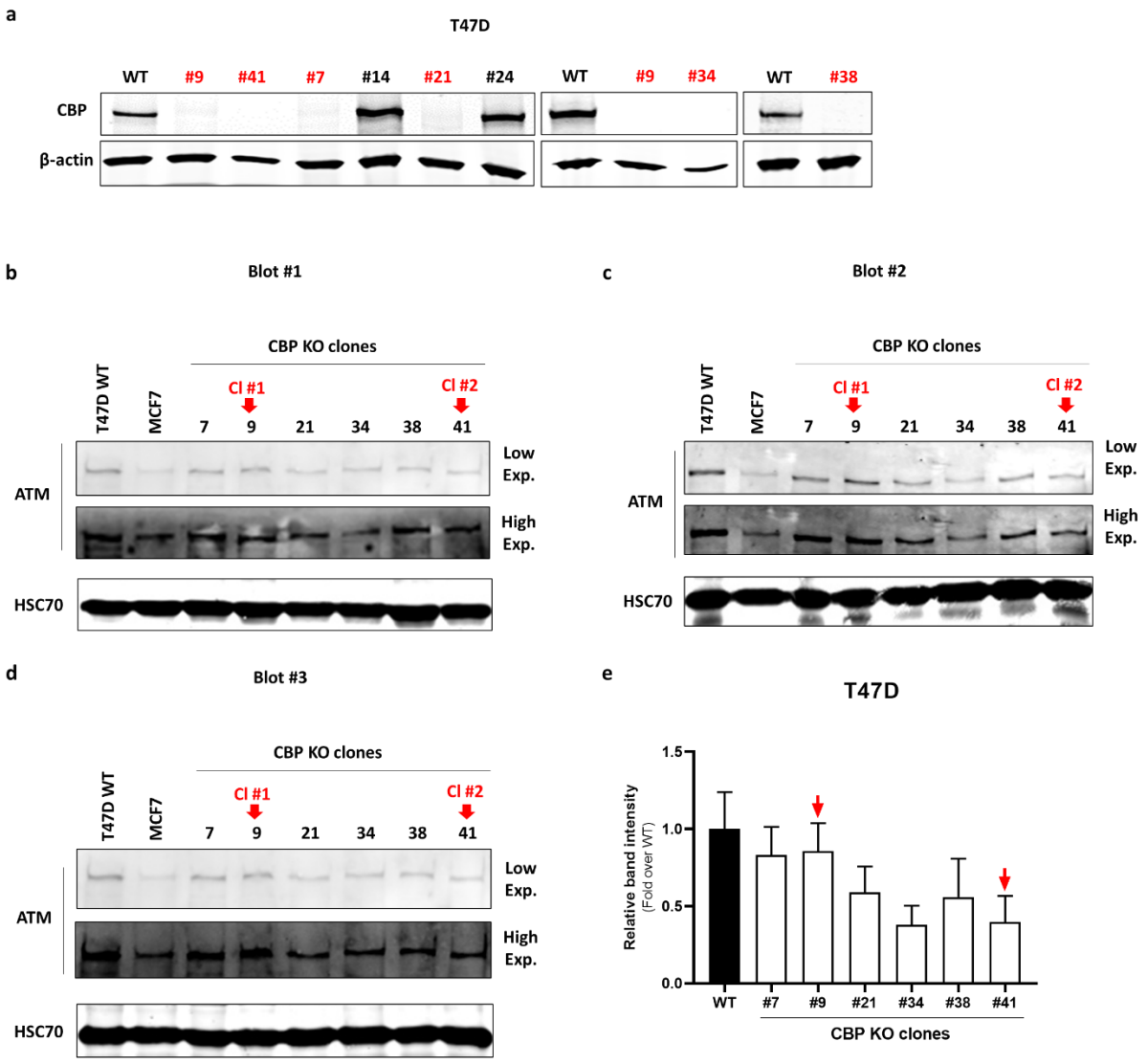

Fig. S4 Screening of CBP and ATM expression in different CBP knockout clones. a Western blot analysis of CBP expression in T47D wild-type (WT) and CRISPR-Cas9 generated CBP knockout (KO) clones, with the KO clones highlighted in red. **b-d** Three independent experiments showing the expression of ATM in T47D WT and six CBP KO clones. Both low (Low Exp.) and high (High Exp.) exposure images are shown. **e** Quantification of ATM band intensities in WT and CBP KO T47D cells, normalized to HSC70 as the loading control. Data are represented as mean ± SEM, n=3.

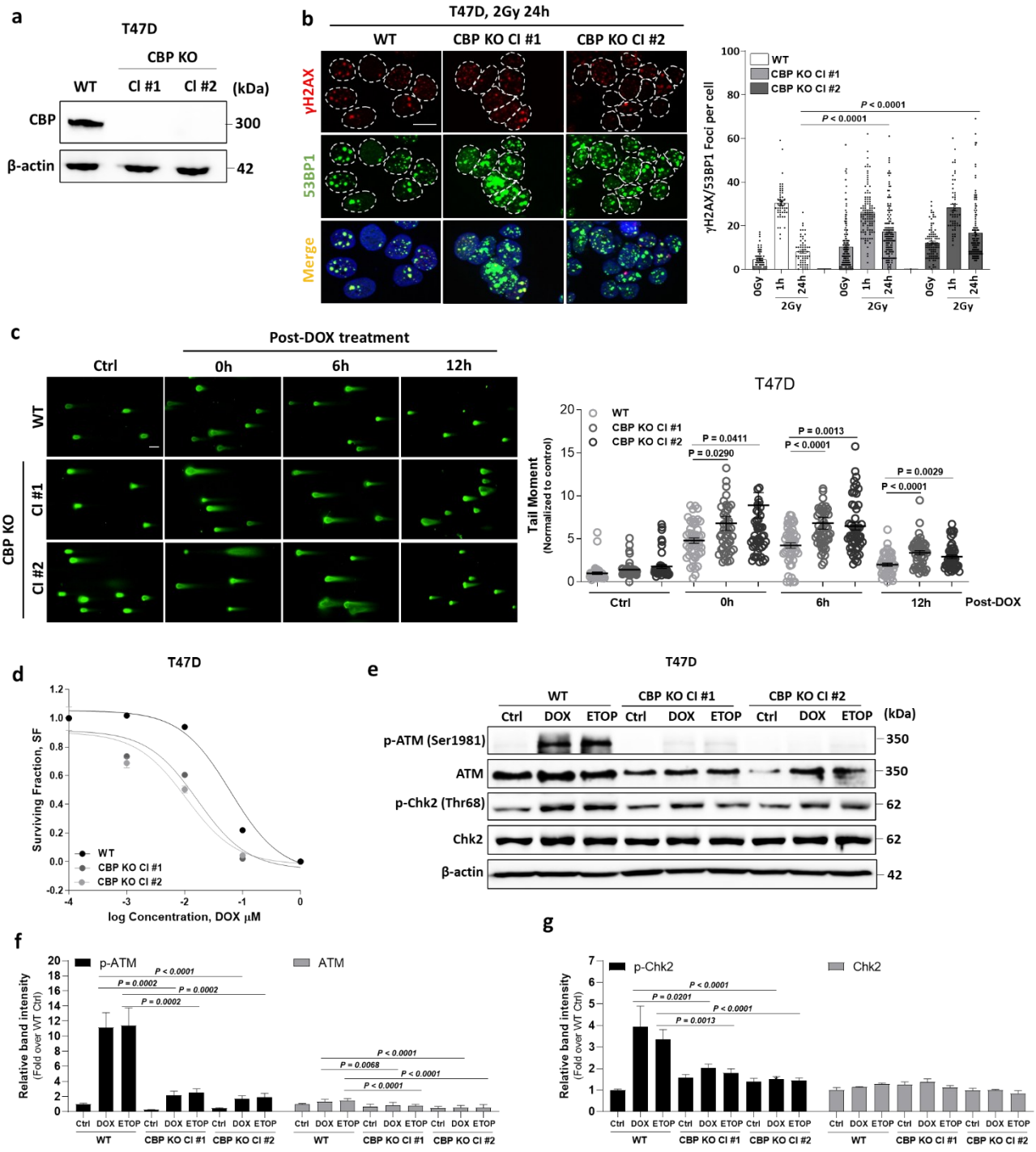

Fig. S5 CBP knockout cells are sensitive to DNA damaging agents and are defective in DNA repair. a Representatives immunoblot analysis of CBP protein expression in T47D CBP knockout (KO) clones #1 and #2 vs wild-type (WT) T47D cells. **b** Left panel: Colocalization of γH2Ax (red) with 53BP1 (green) nuclear foci at 24h after 2Gy ionizing radiation (IR) in T47D WT and CBP KO clones. Scale bar, 100μm. Right panel: Quantification of colocalized γH2Ax with 53BP1 foci at 1 and 24h post-IR from 100 cells. **c** Left panel: Neutral Comet assay images after Doxorubicin (DOX) removal in WT and CBP KO T47D cells. Scale bar, 50μm. Right panel: Fold change of

tail moment at the indicated time points post-DOX incubation from 50 cells, n=3. **d** Clonogenic cell survival assay of T47D WT and CBP KO cells after incubation with DOX. **e** The level of p-ATM, ATM, p-Chk2 and Chk2 in T47D WT and CBP KO clones after incubation with 5μM of DOX or Etoposide (ETOP) for 8h. **f** and **g** Densitometric analysis of protein levels of p-ATM and ATM (**f**) and p-Chk2 and Chk2 (**g**), normalized to β-actin. Data are represented as mean ± SEM, n=3. $P < 0.05$ is considered significant, Mann–Whitney U test.

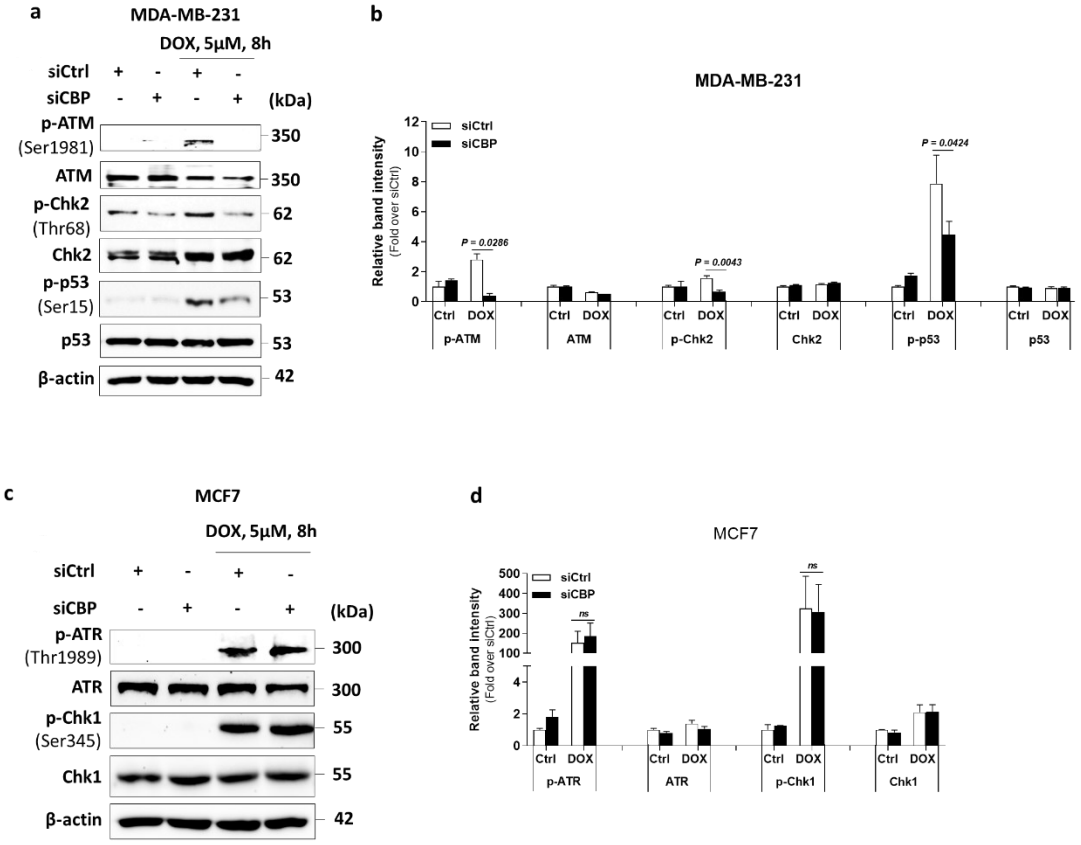

Figure S6 Phosphorylation of ATM/Chk2 and ATR/Chk1 axis under DNA damage in MDA-MB-231 and MCF7 cells after CBP depletion. a Immunoblotting analysis for the phosphorylated and total protein levels of ATM, Chk2 and p53 in MDA-MB-231 cells transfected with the indicated siRNAs followed by Doxorubicin (DOX) treatment. **b** Graph for band quantification of the indicated proteins, normalized to β-actin. The values were normalized to the corresponding untreated siCtrl condition. **c** The levels of p-ATR, ATR, p-Chk1 and Chk1in MCF7 cells transfected with negative control siRNA (siCtrl) or CBP siRNA (siCBP) followed by DOX treatment. **d** Densitometric quantification of the band intensities of the indicated proteins, normalized to β-actin. Data are represented as mean ± SEM, n=2. $P < 0.05$ is considered significant, Mann–Whitney U test.

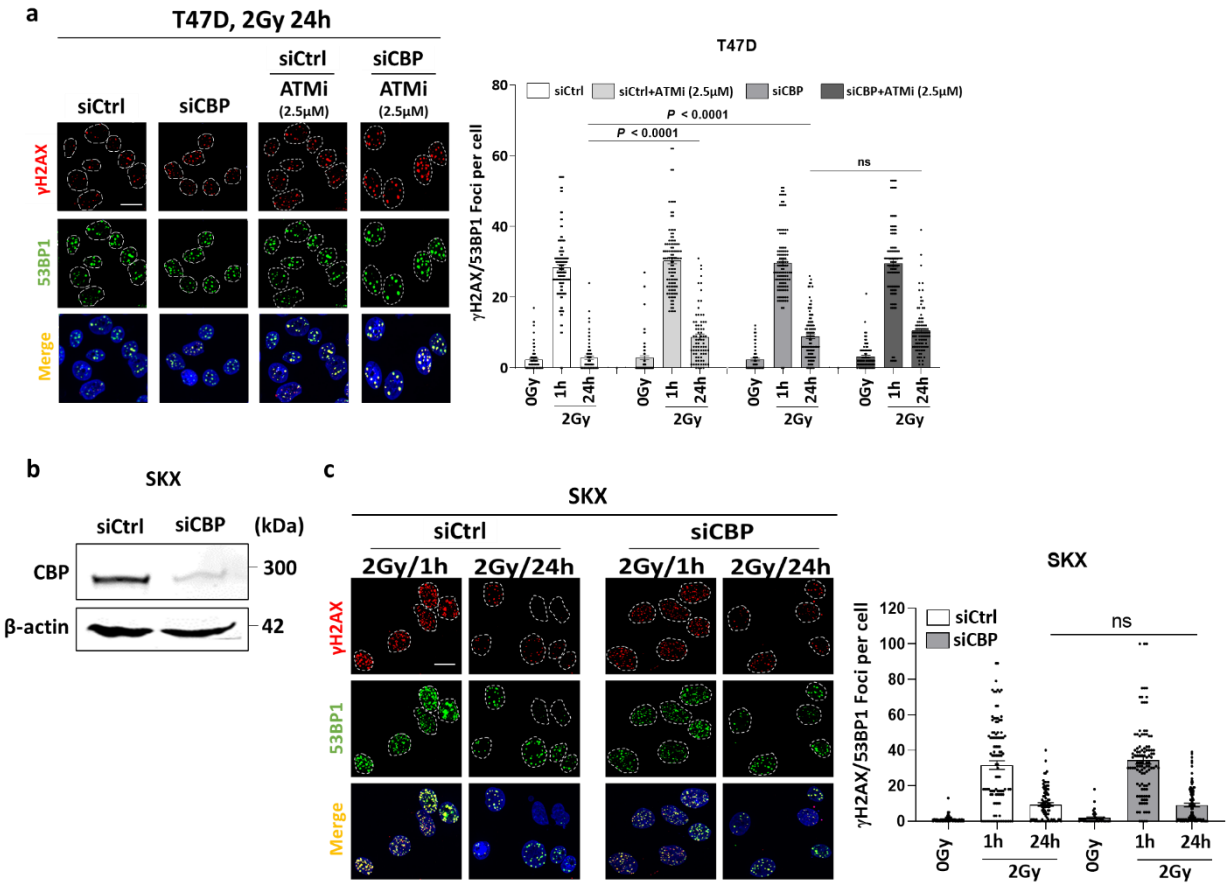

Fig. S7 DNA double strand breaks repair efficiency in T47D and SKX cells after CBP downregulation. a Left panel: Immunofluorescence analysis of γH2Ax (red) and 53BP1 (green) foci in T47D cells transfected with the indicated siRNAs, 24h after 2Gy ionizing radiation (IR) and incubation with 2.5μM of ATM inhibitor (ATMi). Scale bar, 100μm. Right panel: Quantification of γH2Ax/53BP1 foci at 1 and 24h post-IR from 100 cells. **b** Validation of siRNA-mediated depletion of CBP protein in SKX cells. **c** Left panel: Immunofluorescence of γH2Ax (red) and 53BP1 (green) foci in irradiated SKX cells transfected with control or CBP siRNAs. Scale bar, 100μm. Right panel: The average colocalized γH2Ax/53BP1 foci were counted from 100 cells and presented in a bar graph. Data are represented as mean ± SEM, n=3. $P < 0.05$ is considered significant, Mann–Whitney U test. ns, not significant.

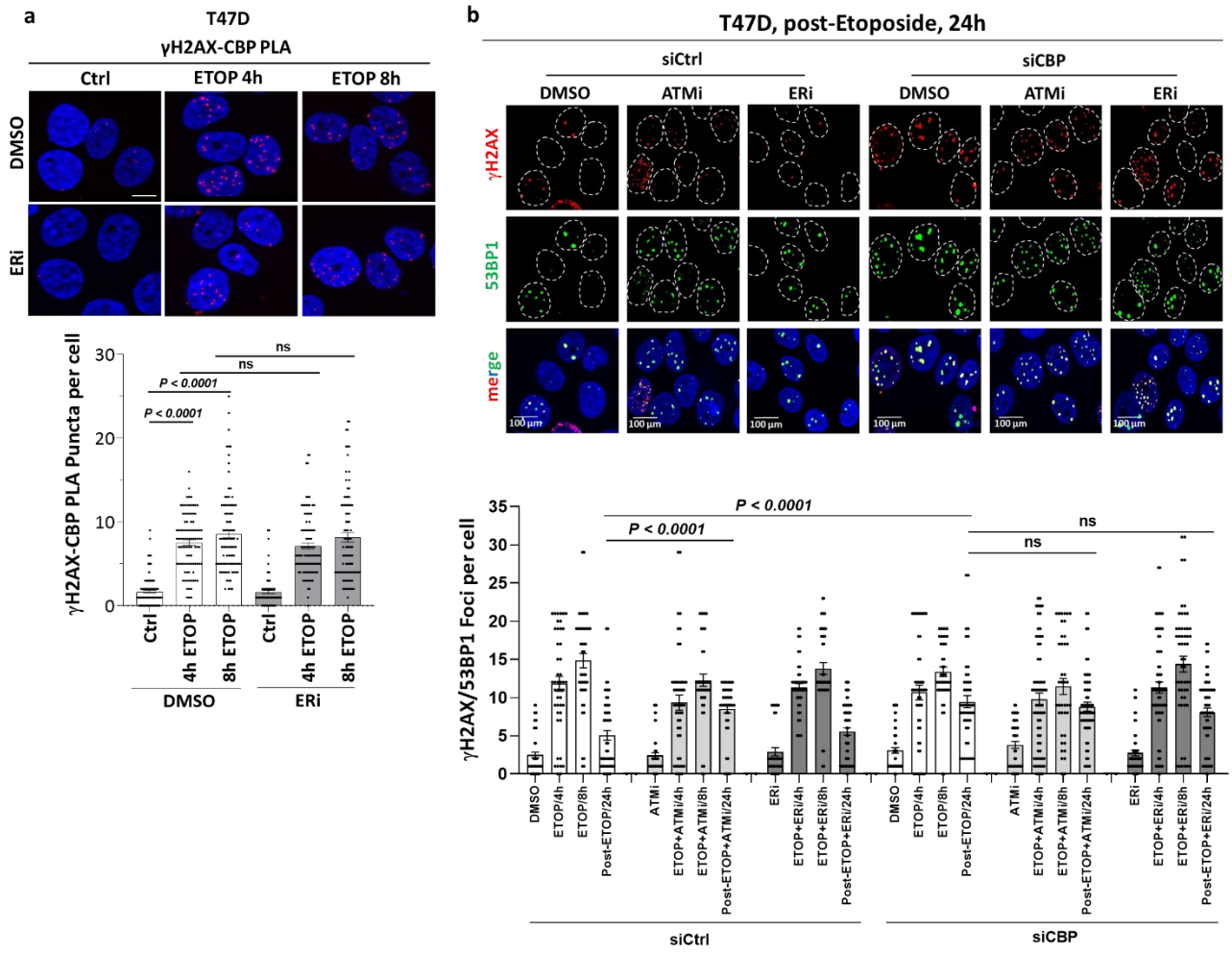

Fig. S8 ER-independent role of CBP in the response of T47D cells to Etoposide-induced DNA damage. a Upper panel: Proximity ligation assay (PLA) for colocalization of γH2Ax and CBP in T47D cells after incubation with estrogen receptor inhibitor (ERi) for 4h, followed by incubation with Etoposide (ETOP) for the indicated time points. Scale bar, 100µm. Lower panel: Quantification of PLA signals for γH2Ax and CBP using ImageJ software from 100 cells. **b** Upper panel: Colocalization of γH2Ax (red) with 53BP1 (green) nuclear foci in T47D cells transfected with negative control (siCtrl) or CBP (siCBP) siRNA after ETOP removal. Scale bar, 100µm. Lower panel: Bar graphs representing the quantification of colocalized foci from 100 cells. Data are represented as mean ± SEM, n=3. $P < 0.05$ is considered significant, Mann–Whitney U test. ns, not significant.

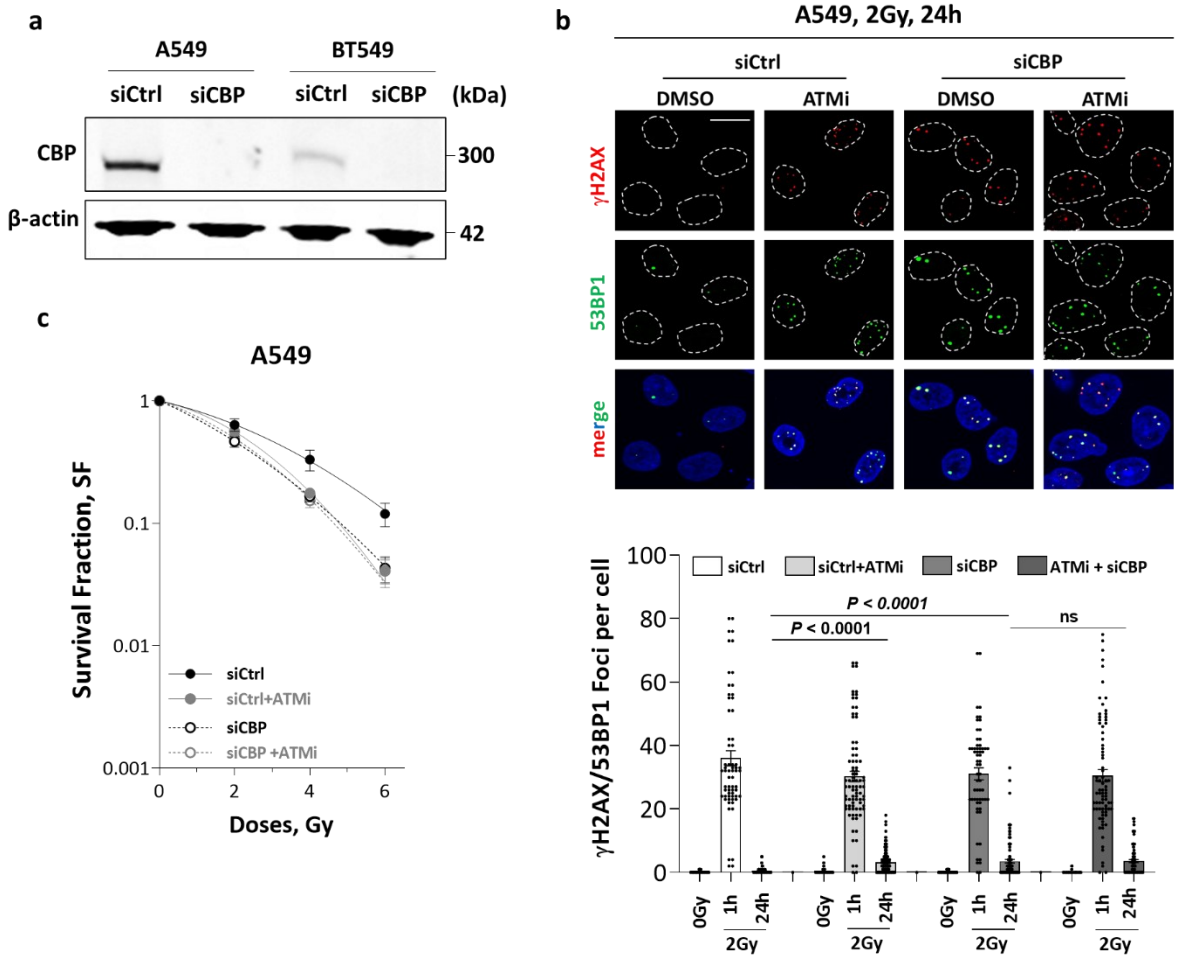

Fig. S9 Involvement of CBP in DNA damage response in lung cancer A549 cells. a Validation of siRNA-mediated depletion of CBP protein in A549 and BT549 cells. **b** Upper panel: Representative immunofluorescence images for γH2Ax (red) and 53BP1 (green) foci in A549 cells transfected with the indicated siRNAs, after incubation with 5μM of ATM inhibitor (ATMi) at 24h post-2Gy ionizing radiation (IR). Scale bar, 100μm. Lower panel: Quantification analysis of γH2Ax/53BP1 foci at 1 and 24h post-IR from 100 cells. **c** Colony formation assay of transfected A549 cells with the indicated siRNA, treated with and without 2.5μM ATMi before irradiation. Data are represented as mean ± SEM, n=3. $P < 0.05$ is considered significant, Mann–Whitney U test. ns, not significant.

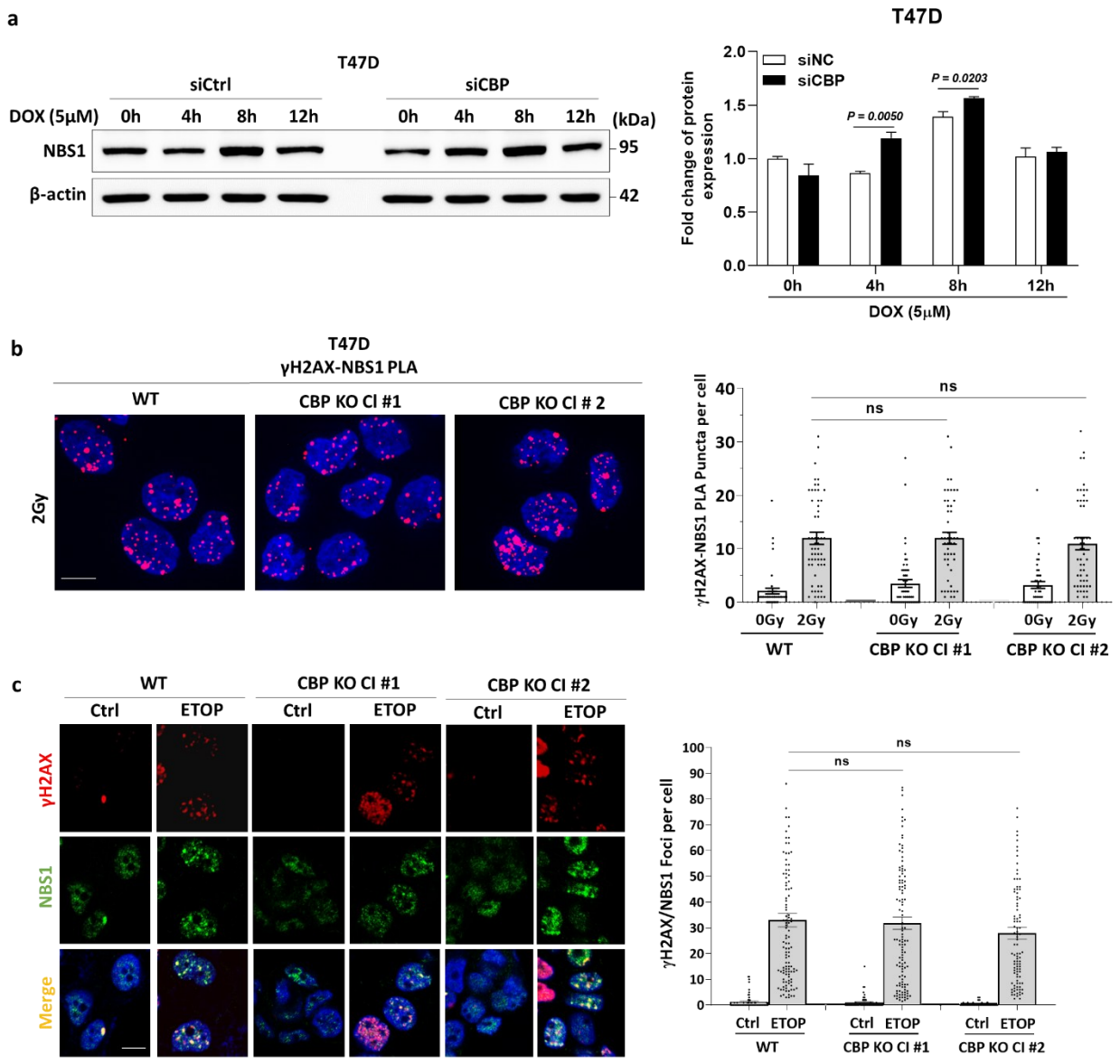

Fig. S10 Stability and recruitment of NBS1 in CBP-depleted cells after DNA damage induction. a Left panel: Immunoblot analysis for NBS1 levels in T47D cells transfected with siCBP or siNC, treated with 5μM of Doxorubicin (DOX) for indicated time points. Right panel: Densitometric quantification of NBS1 levels normalized to β-actin. The fold change was calculated relative to the siCtrl 0h sample. **b** Left panel: Proximity ligation assay (PLA) showing γH2Ax and NBS1 colocalization in T47D wild-type (WT) and CBP knockout (KO) clones, 5mins post 2Gy ionizing radiation (IR). Right panel: Quantification of PLA signals from 100 cells. **c** Left panel: Representative immunofluorescence images for γH2Ax (red) and NBS1 (green) foci in T47D WT and CBP KO clones, after incubation with 5μM Etoposide (ETOP) for 8h. Scale bar, 100μm. Right panel: Quantification of γH2Ax/NBS1 foci in the WT and KO clones from 100 cells. Data are represented as mean ± SEM, n=2. $P < 0.05$ is considered significant, Mann–Whitney U test. ns, not significant.

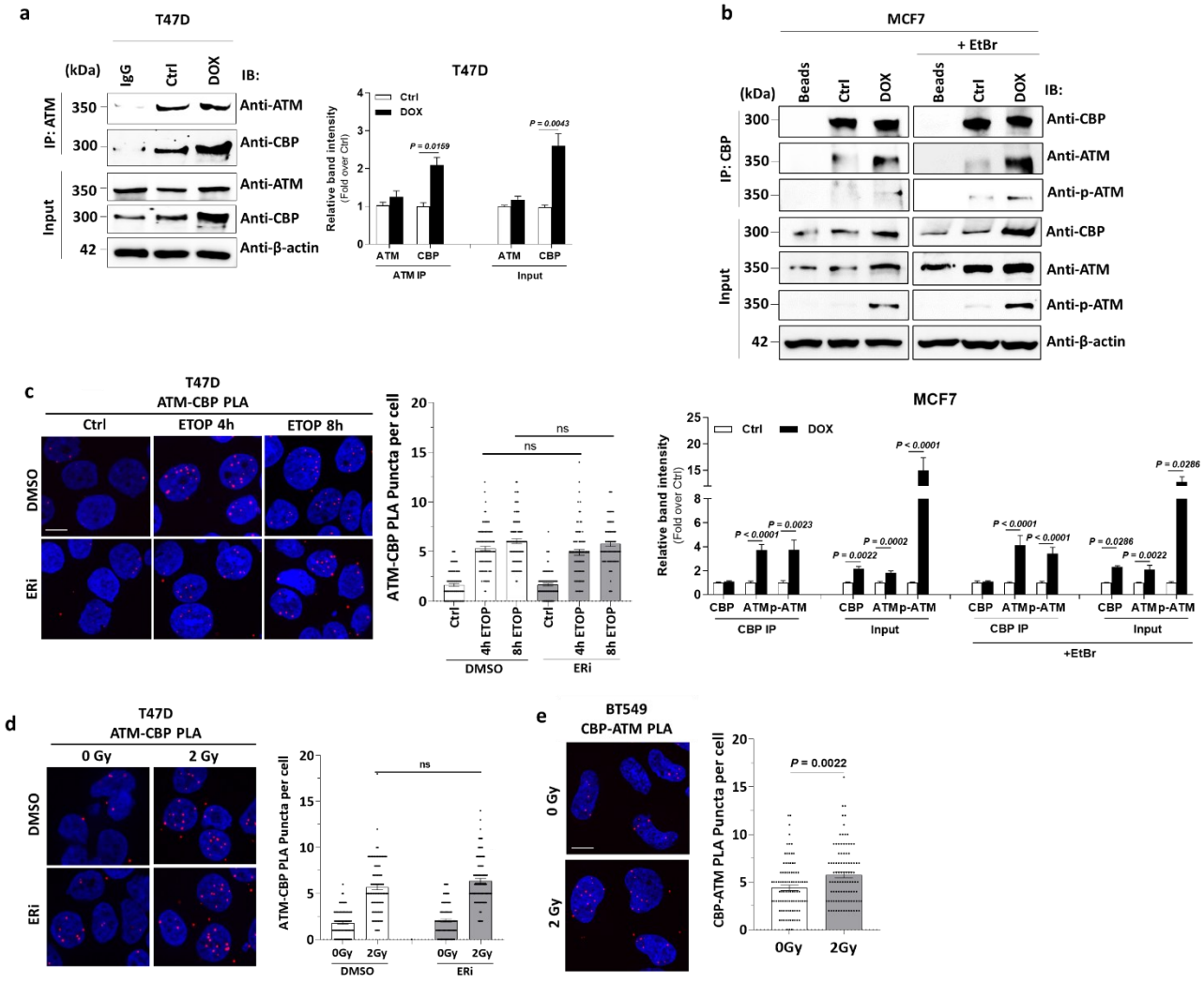

Fig. S11 Interaction between CBP and ATM after DNA damage induction in MCF7, T47D and BT-549 cells. a Left panel: Reciprocal immunoprecipitation (IP) of ATM from T47D cells treated with Doxorubicin (DOX) for 8h. Immunocomplexes were analyzed by immunoblotting with a CBP antibody. Right panel: Graph for densitometric quantification of CBP and ATM in the immunoprecipitated and input samples. **b** Upper panel: MCF7 cells were incubated with 5µM of DOX for 8h. Prior to co-immunoprecipitation, the lysates were treated with and without ethidium bromide (EtBr) to eliminate DNA-dependent protein association. Extracts from treated cells were then immunoprecipitated with an anti-CBP antibody. Lower panel: Band quantification of CBP, ATM and p-ATM levels in both immunoprecipitated and input samples. **c-e** Left panels: Proximity ligation analysis (PLA) of CBP and ATM in T47D cells after incubation with estrogen receptor inhibitor (ERi) for 4h followed by incubation with Etoposide (ETOP) for the indicated time points (**c**), T47D cells after treatment with ERi 4h before irradiation with 2Gy (**d**), and BT-549 cells after 5mins of 2Gy IR (**e**). DAPI staining (blue) showing the nucleus. Scale bar, 100µm. Right panels: Quantification of CBP-ATM PLA signals from 100 cells is shown in graphs. Data are represented as mean ± SEM, n=3. $P < 0.05$ is considered significant, Mann–Whitney U test. ns, not significant.

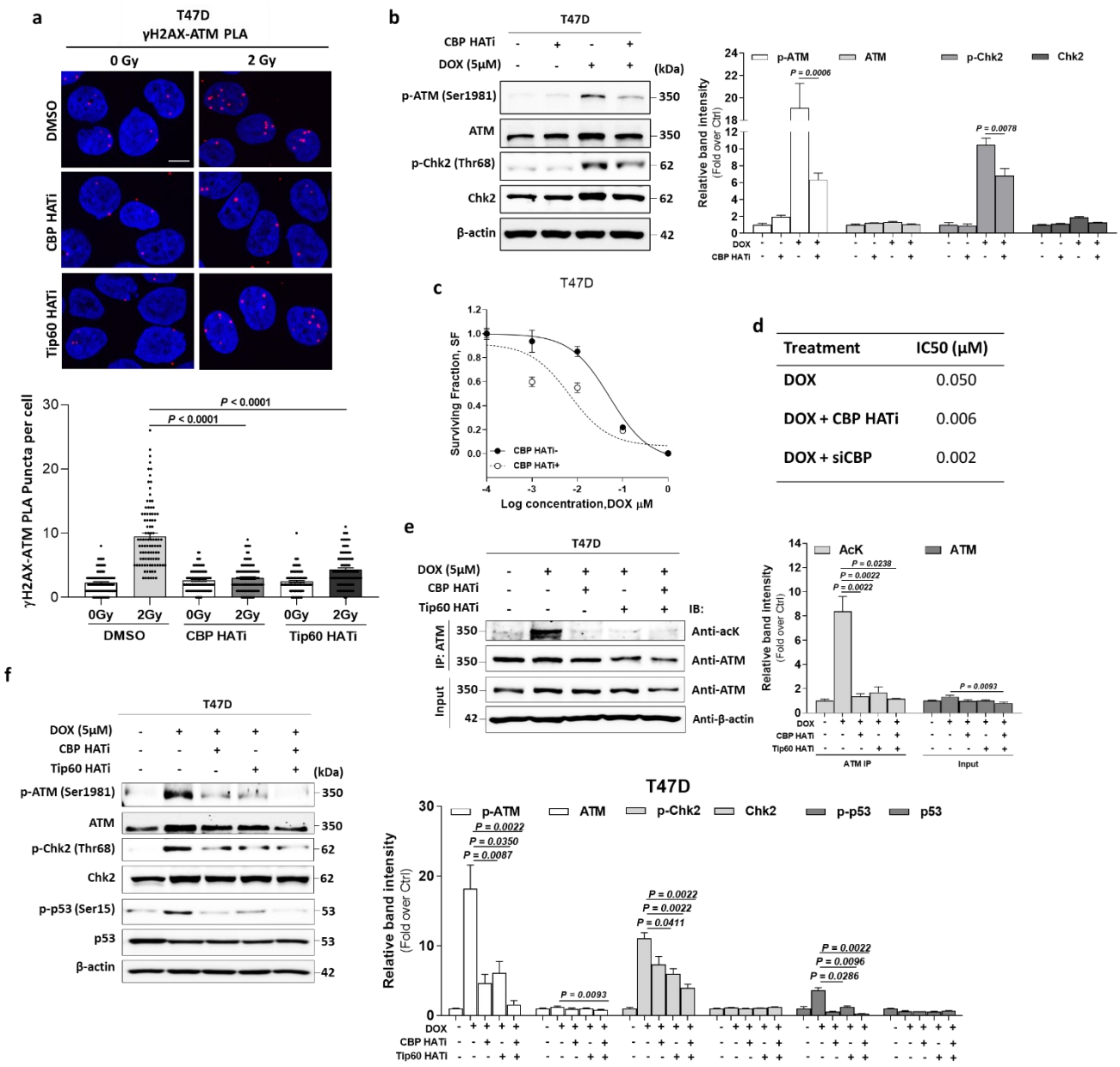

Fig. S12 Inhibition of CBP histone acetyltransferase activity reduces the DNA damage response in T47D cells. a Upper panel: Proximity ligation assay (PLA) of γH2Ax and ATM colocalization in T47D cells incubated with 8μM of CBP HAT inhibitor (CBP HATi) for 24h or 25μM of Tip60 HAT inhibitor (Tip60 HATi) for 1h prior to irradiation with 2Gy. The nucleus was stained with DAPI. Scale bar, 100μm. Lower panel: The graph shows the average of PLA signals per cell counted in 100 cells. **b** Left panel: Immunoblotting analysis of p-ATM, ATM, p-Chk2 and Chk2 following incubation with CBP HATi prior to Doxorubicin (DOX). Right panel: Band quantifications of the indicated proteins after normalization to β-actin and untreated control samples. **c** Colony survival assay of T47D cells after incubation with different concentration of DOX in the presence or absence of CBP HATi. **d** IC50 values for DOX alone or in combination with CBP HATi, as well as for DOX in CBP-downregulated cells**. e** Left panel: Immunoprecipitation of ATM to assess acetylation status (AcK) in T47D cells treated with 5 μM

DOX in the presence or absence of CBP HATi or/and Tip60 HATi. Immunoprecipitated (IP) samples were probed for acetylated lysine (AcK) and ATM using specific antibodies. β-actin was included as a loading control for the input samples. Right panel: Quantification of acetylated ATM (AcK) and total ATM levels from the immunoprecipitation experiment. **f** Left panel: Western blot analysis of T47D cells under the same treatment conditions. Protein levels of p-ATM, ATM, p-Chk2, Chk2, p-p53, p53, and β-actin (loading control) were evaluated. Right panel: Quantification of bands from western blot analysis showing fold changes in protein expression relative to untreated controls. Data are represented as mean ± SEM, n=2. $P < 0.05$ is considered significant, Mann–Whitney U test.

Fig. S13

(a) Raw data for Fig. 1a

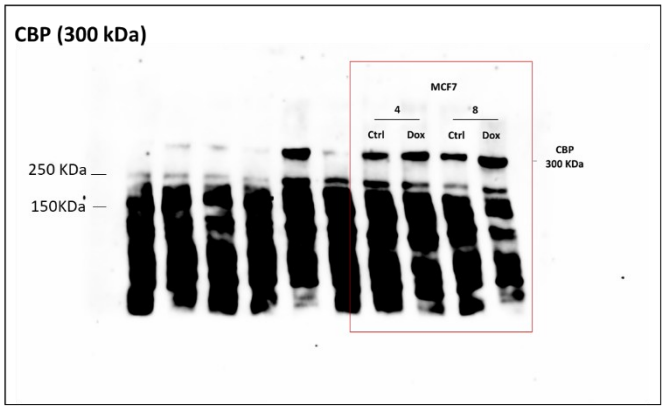

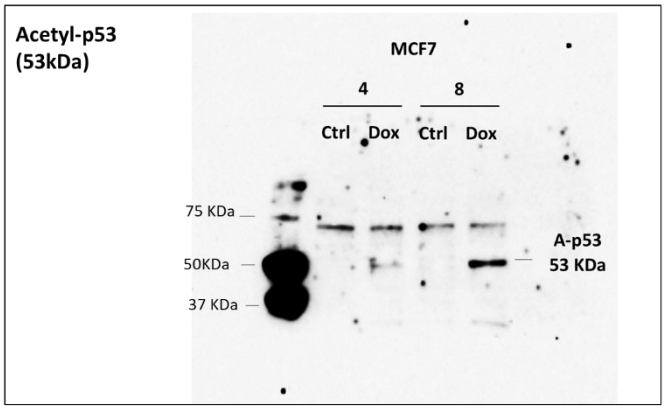

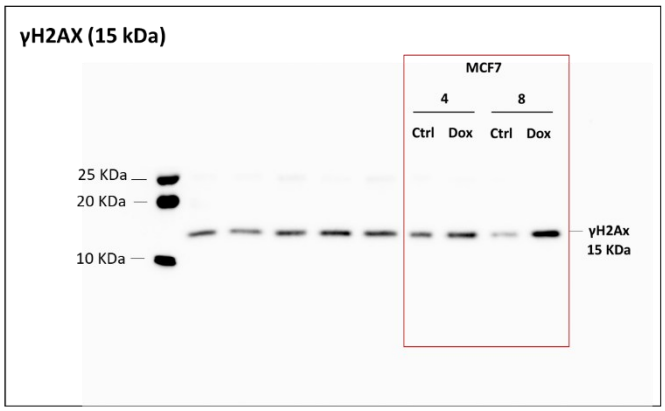

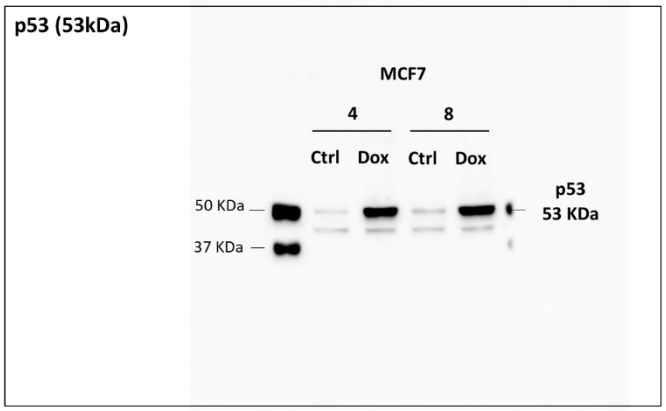

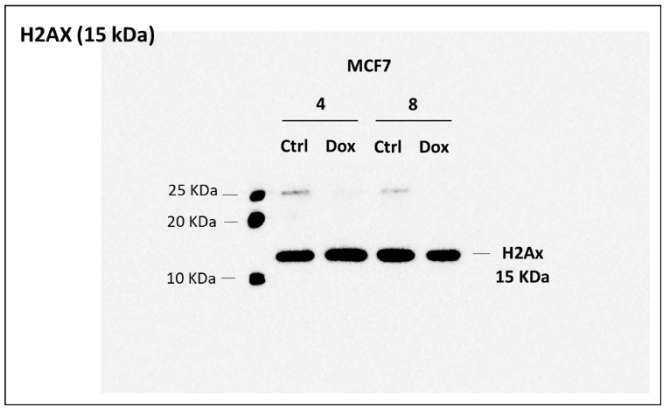

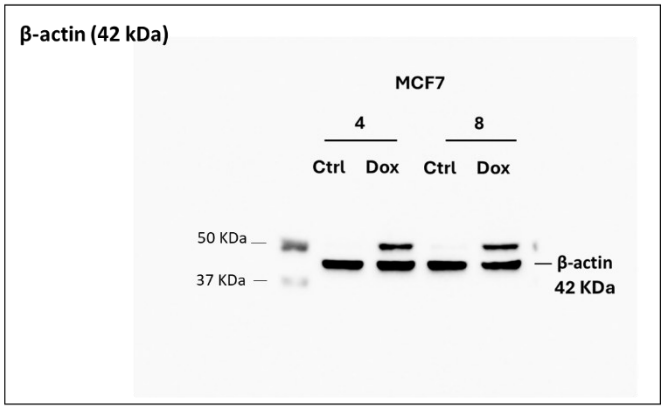

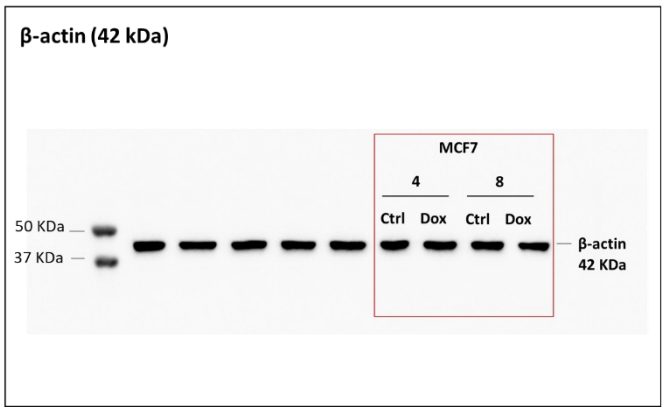

Fig. S13

(a) Raw data for Fig. 1a

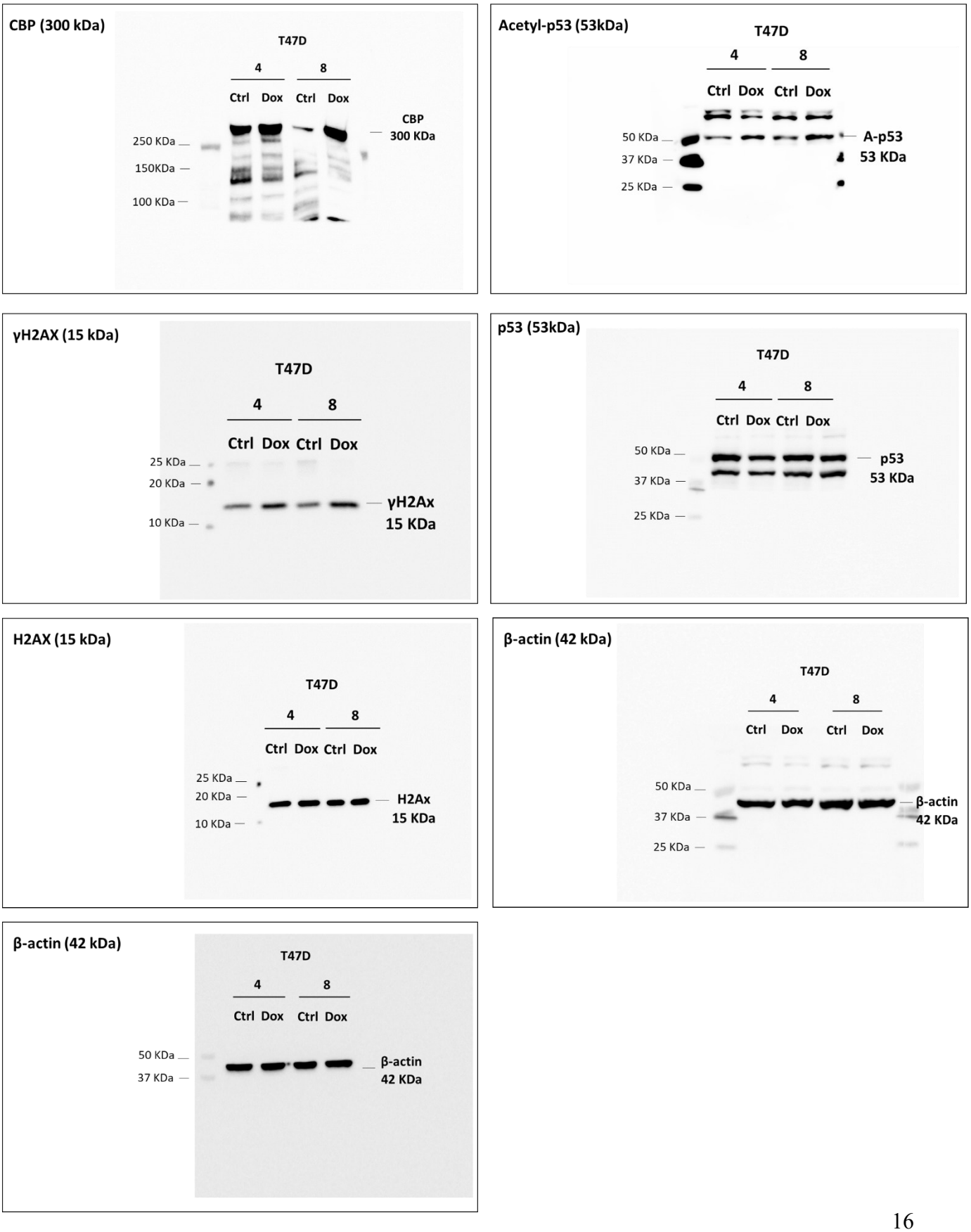

Fig. S13

(b) Raw data for Fig. 1d

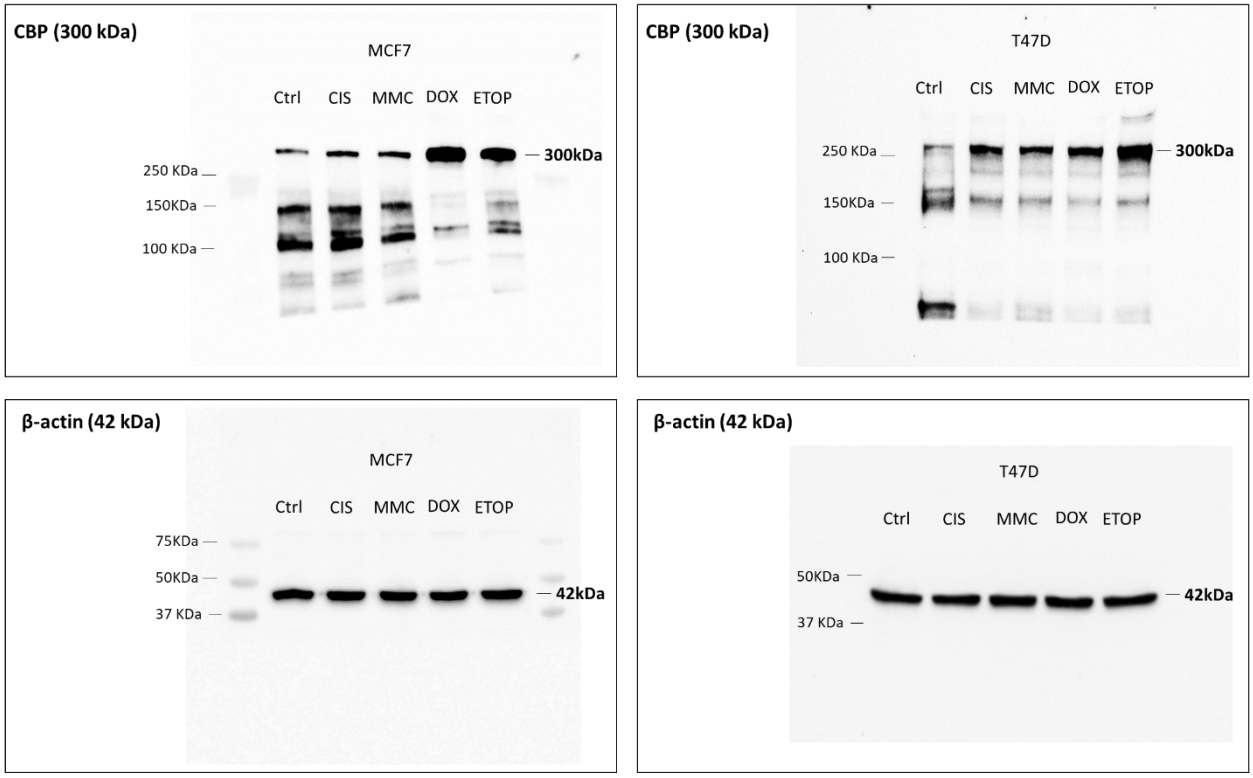

Fig. S13

(c) Raw data for Fig. 3a

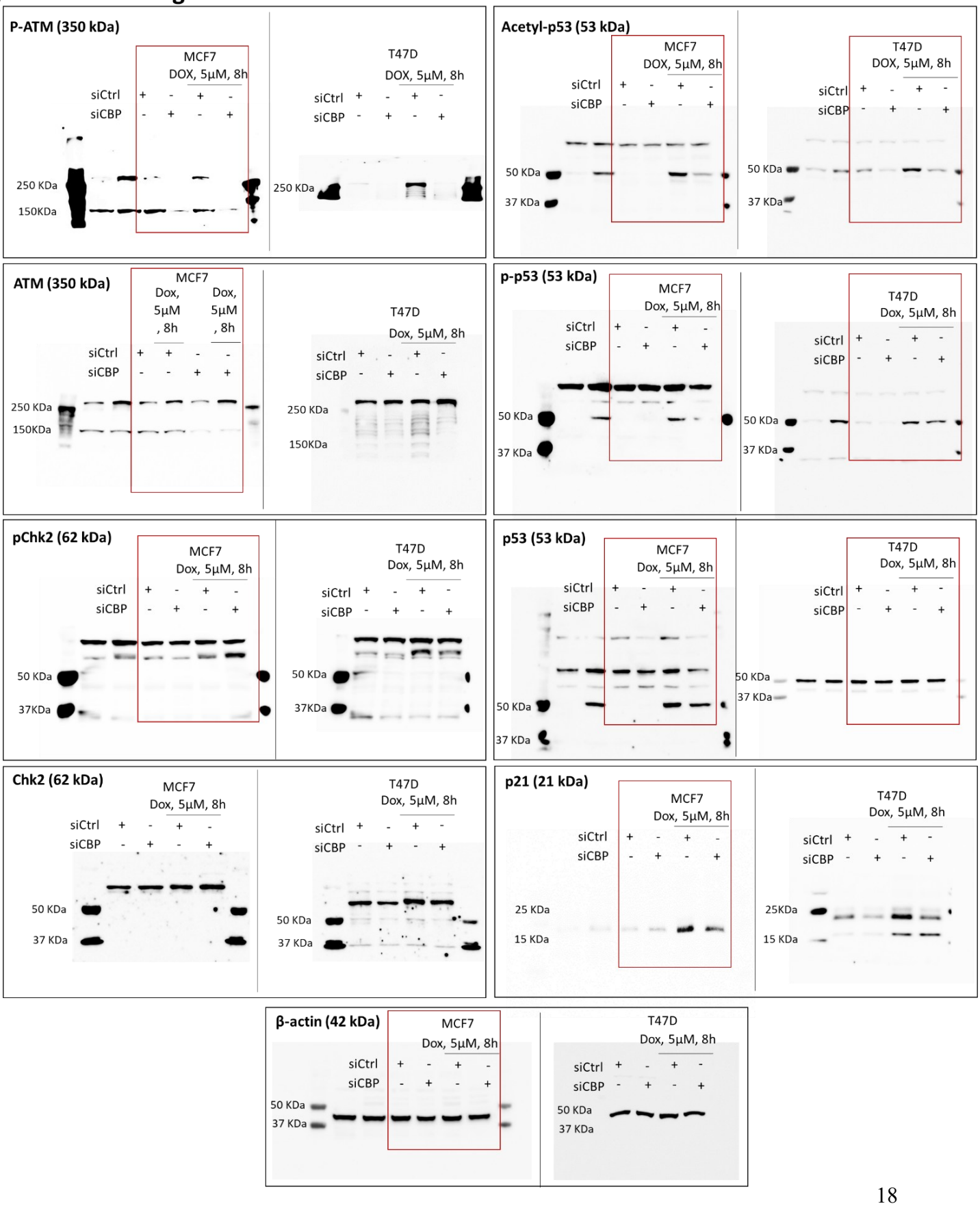

Fig. S13

(d) Raw data for Fig. 6c

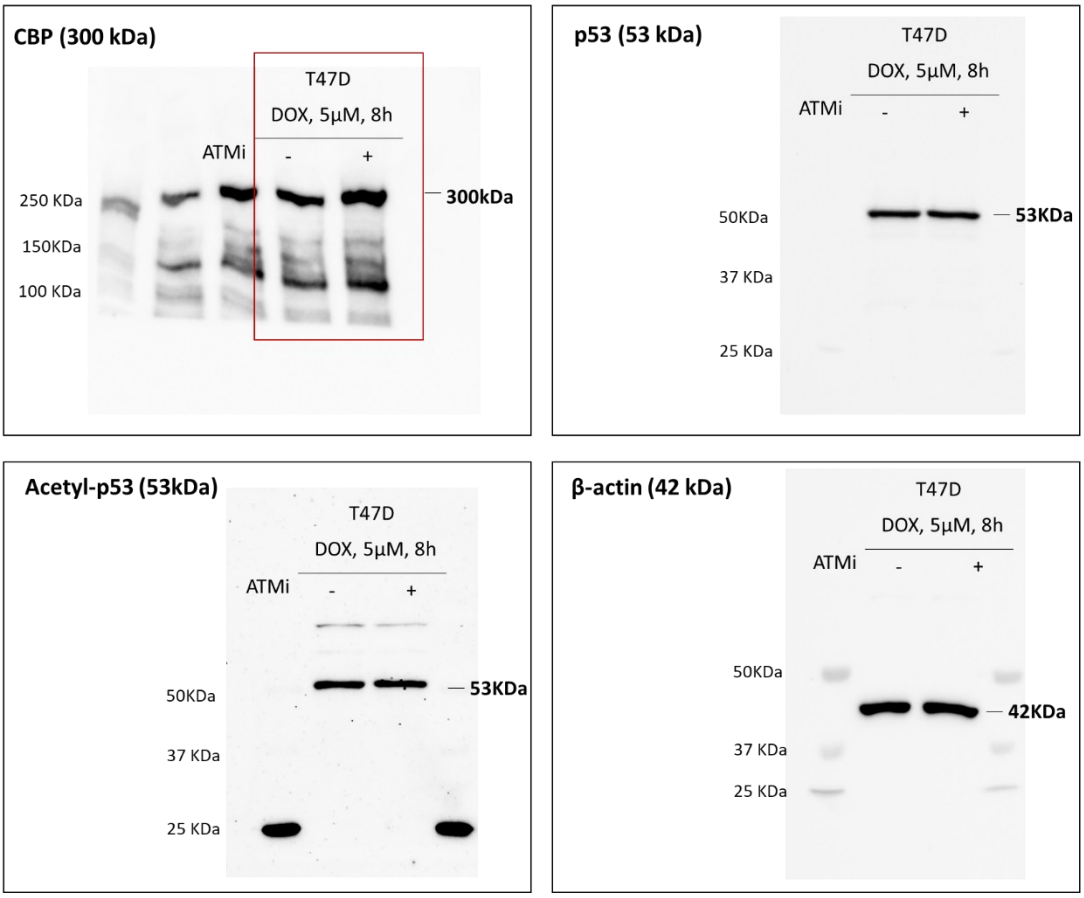

Fig. S13

(e) Raw data for Fig. 7a

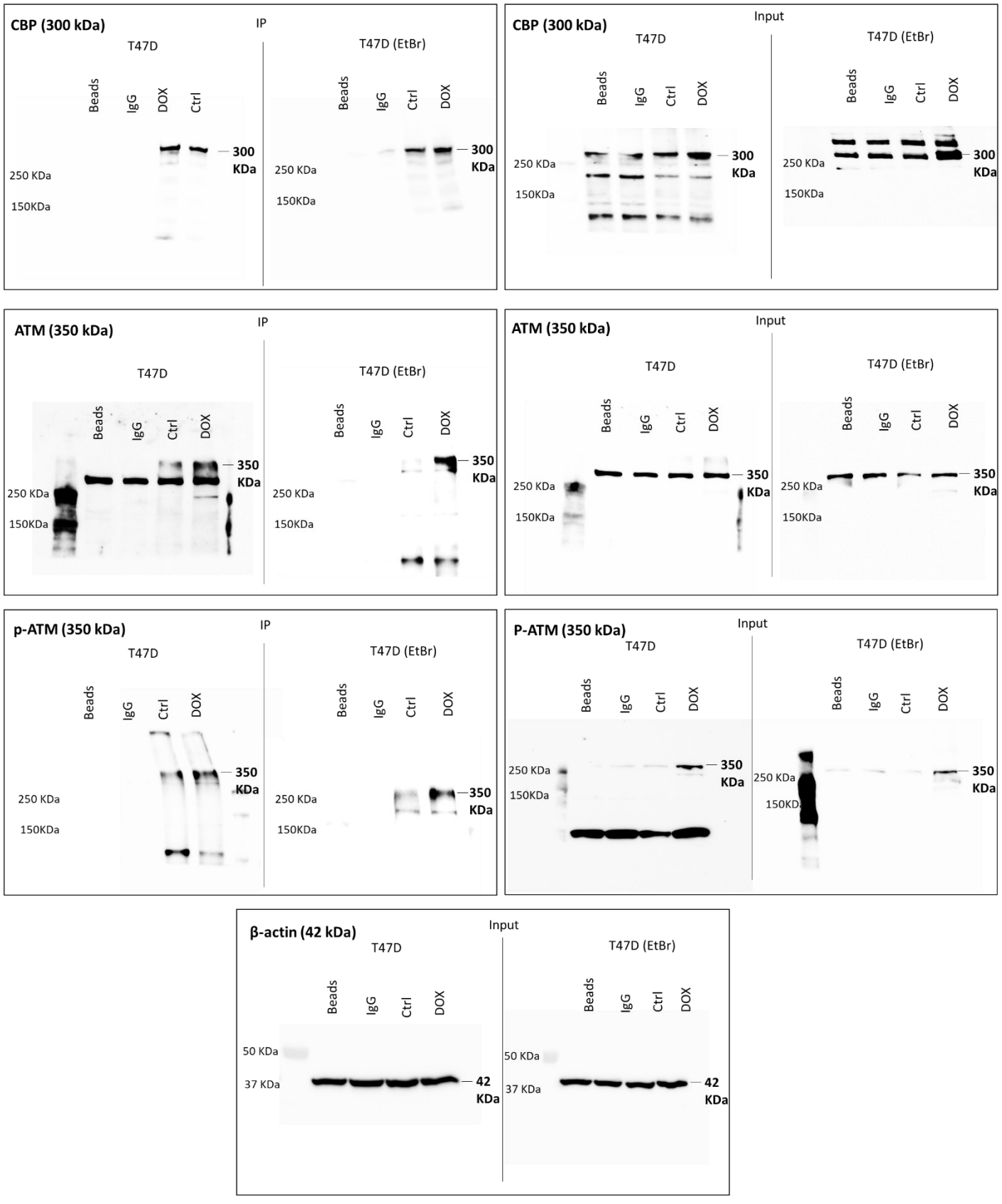

Fig. S13
(f) Raw data for Fig. 7d

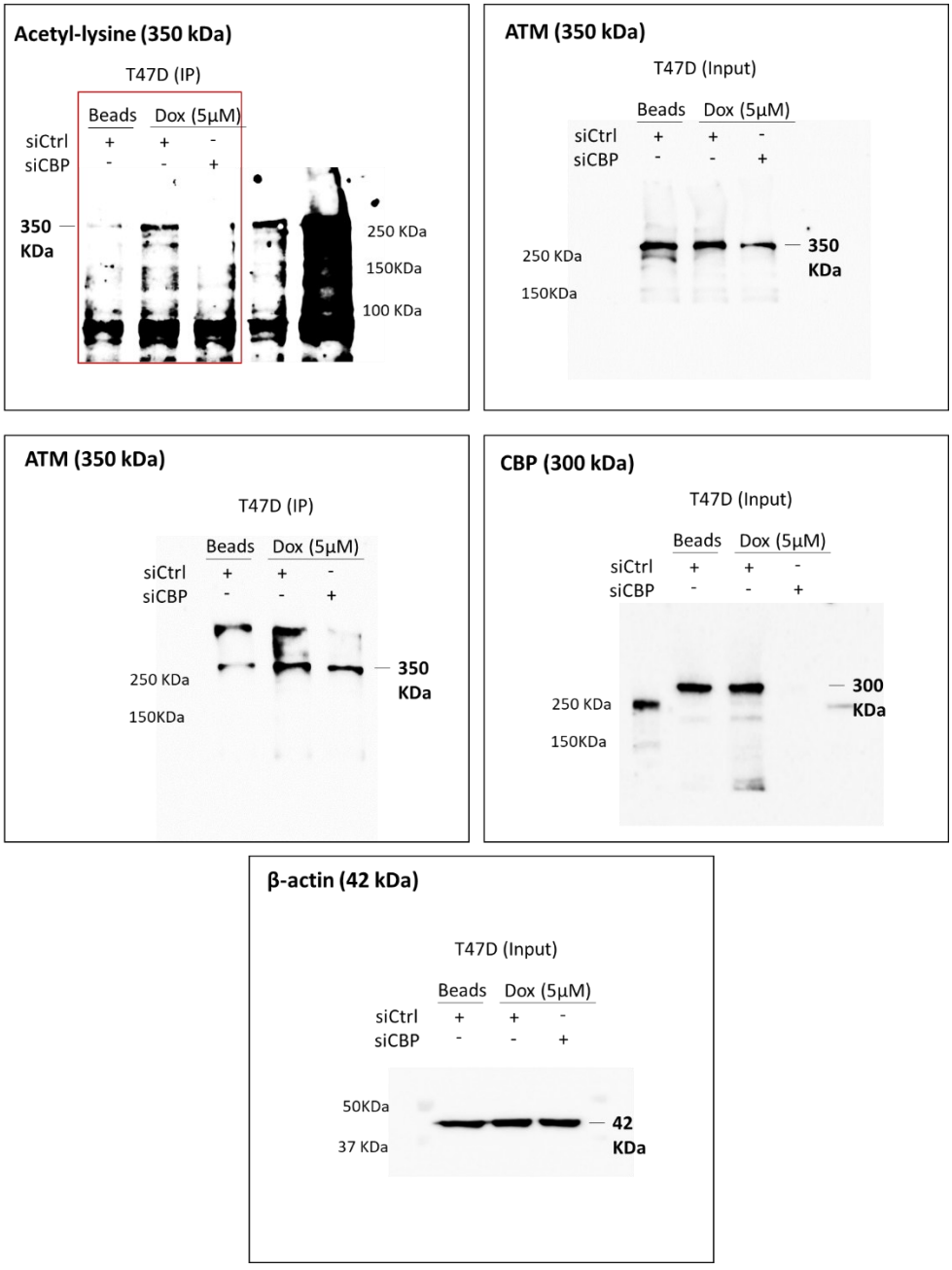

Fig. S13

(g) Raw data for Fig. 7f

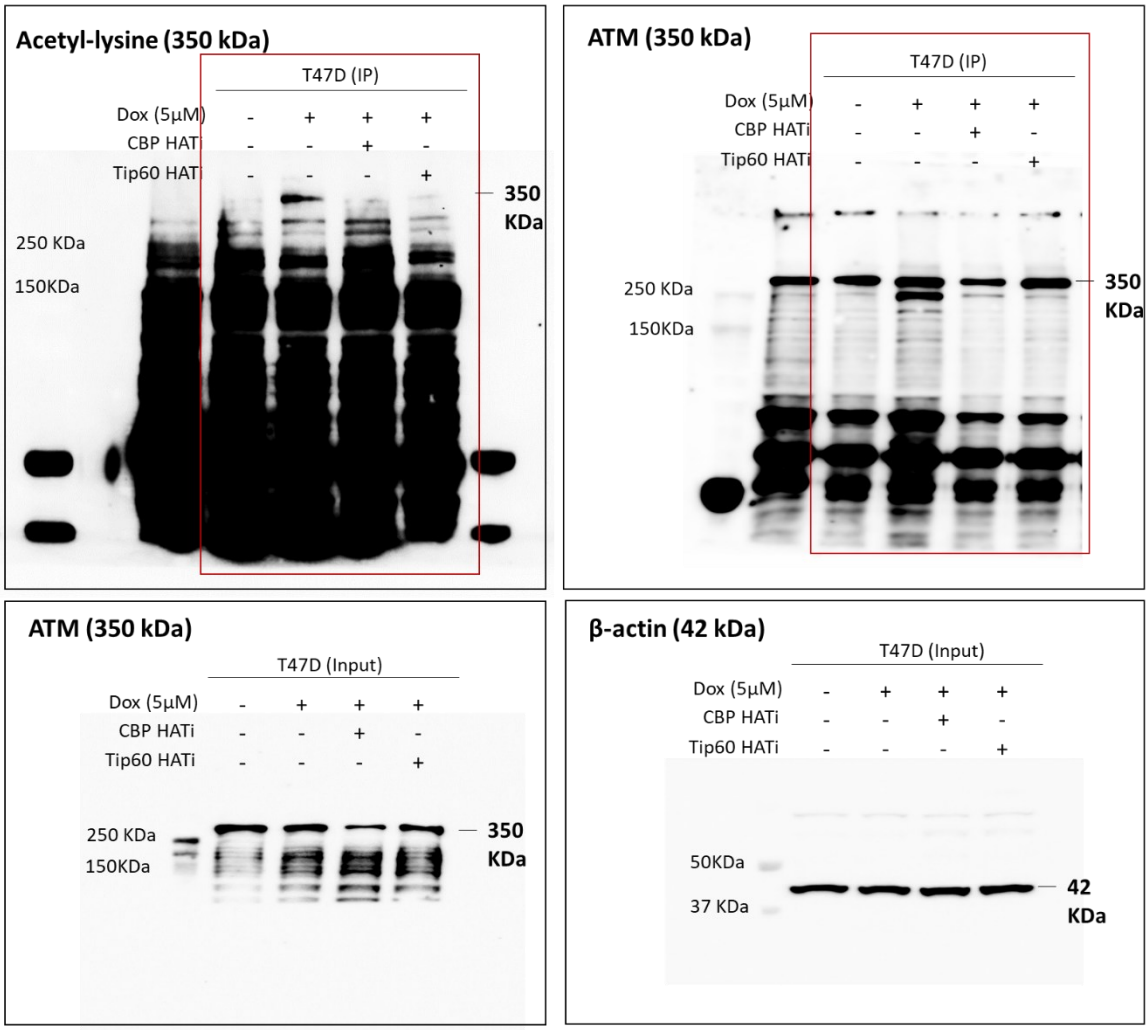

Fig. S13

(h) Raw data for Fig. S1b

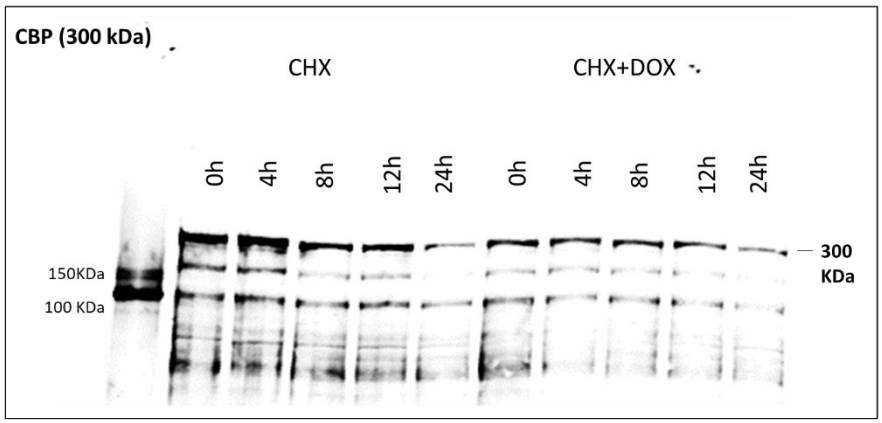

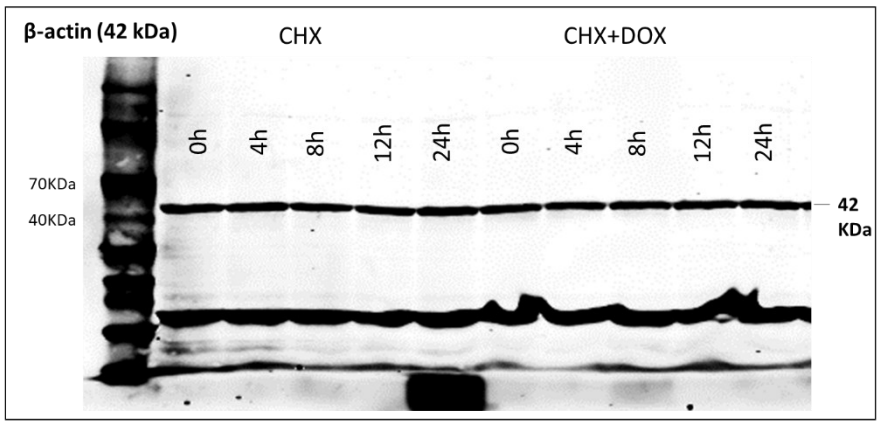

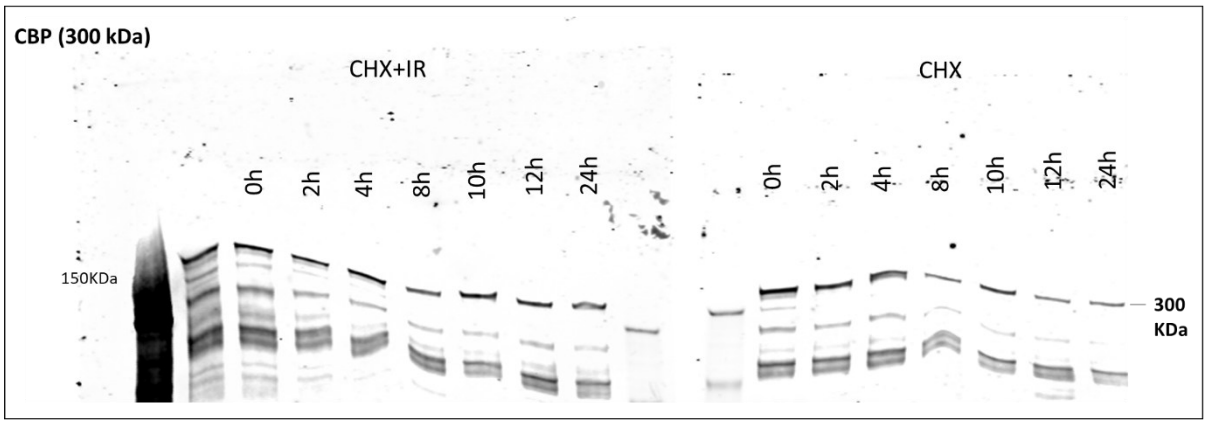

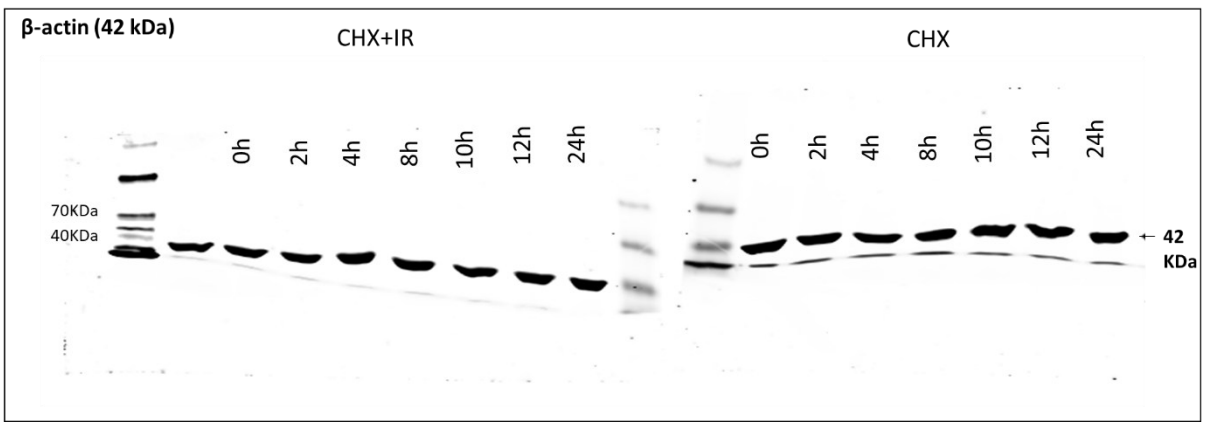

Fig. S13

(i) Raw data for Fig. S2f

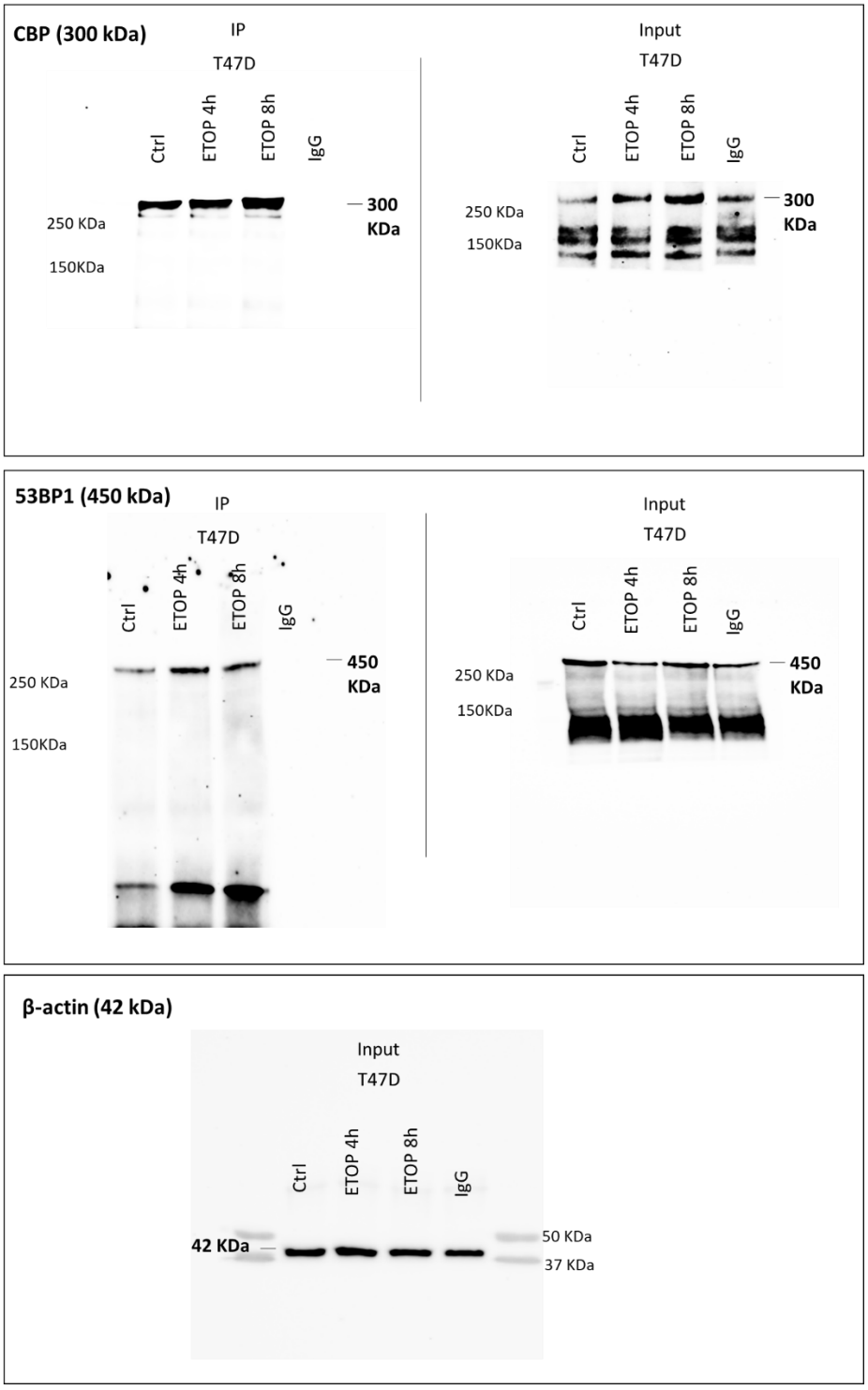

Fig. S13

(j) Raw data for Fig. S3a

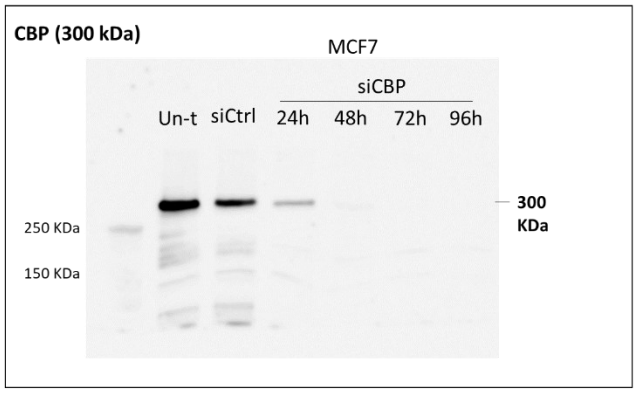

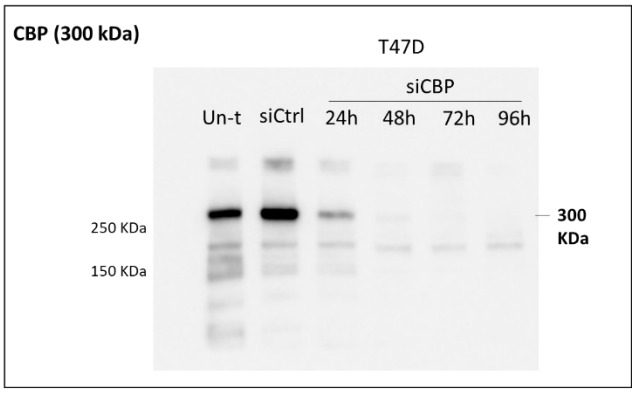

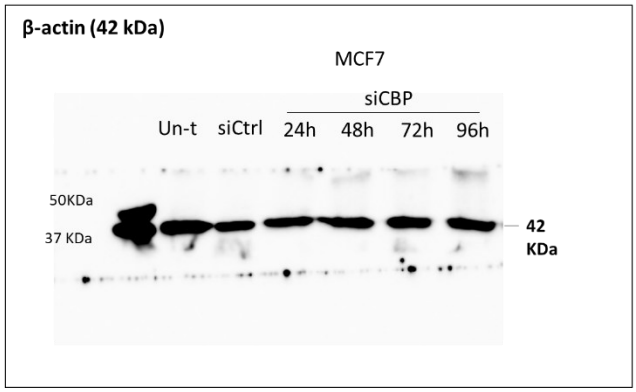

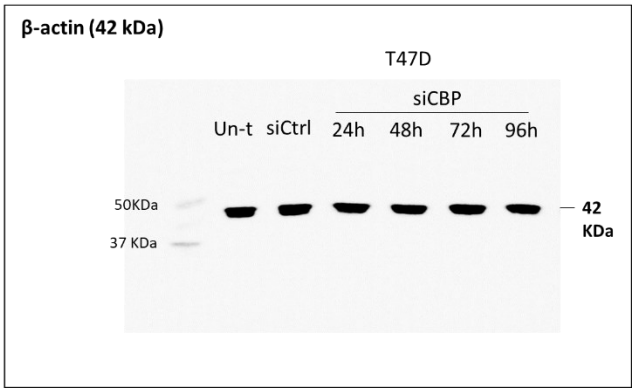

Fig. S13

(k) Raw data for Fig. S4a

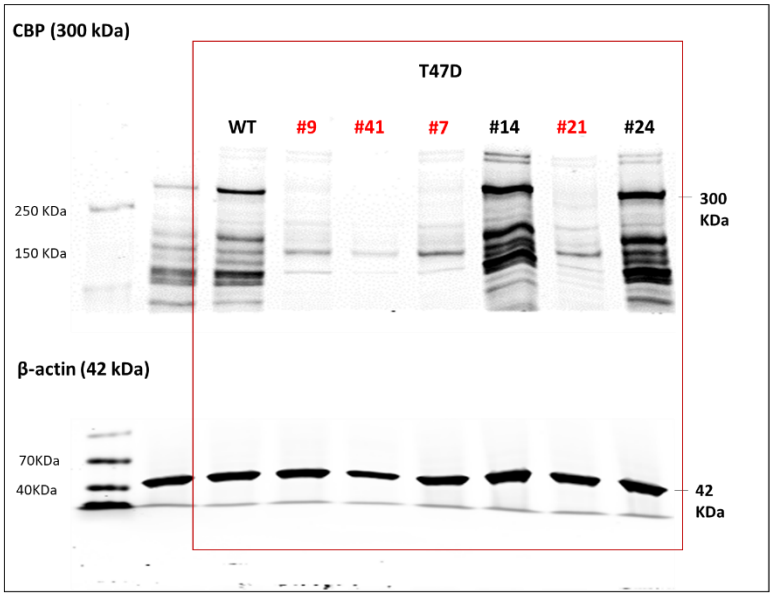

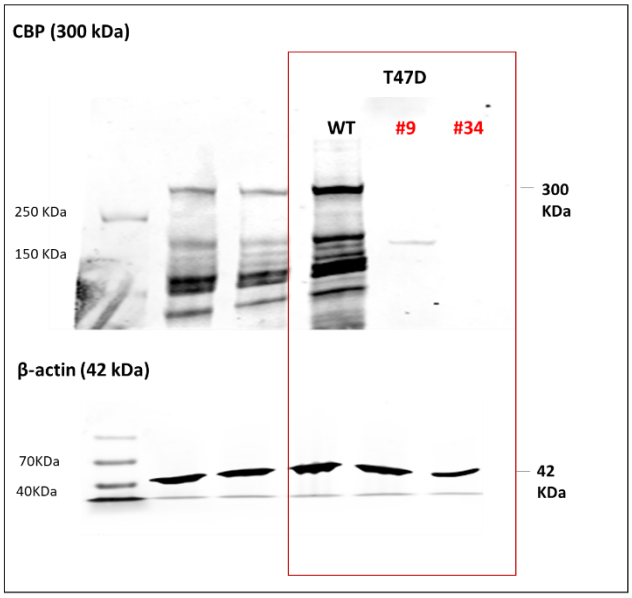

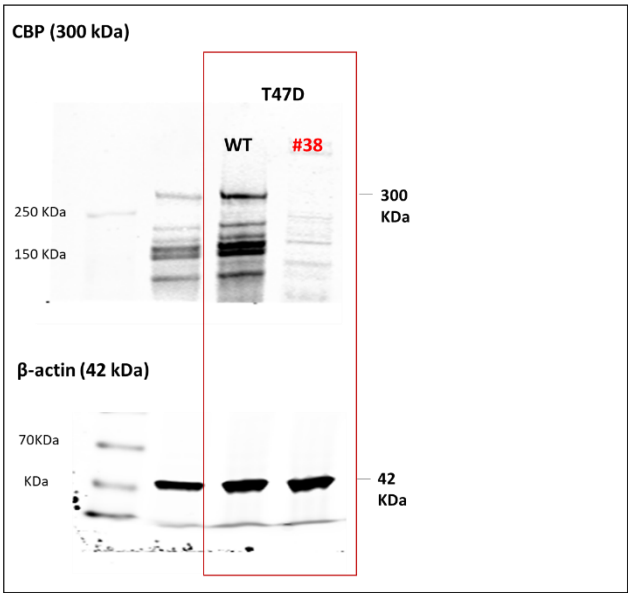

Fig. S13

(l) Raw data for Fig. S4b

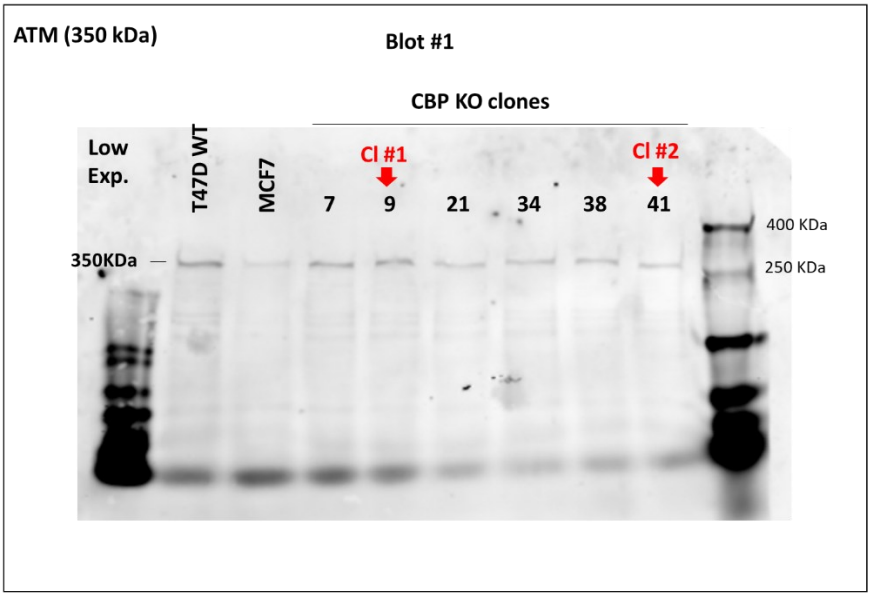

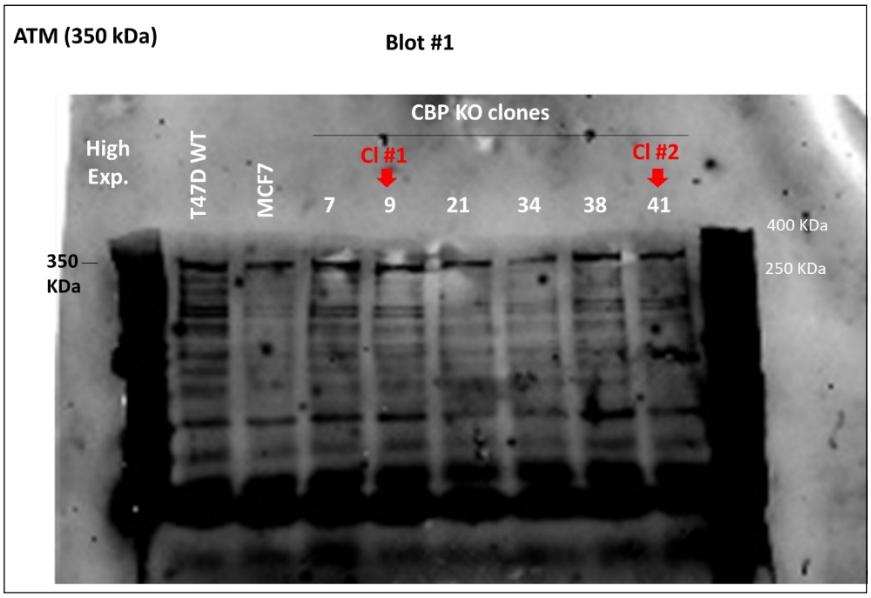

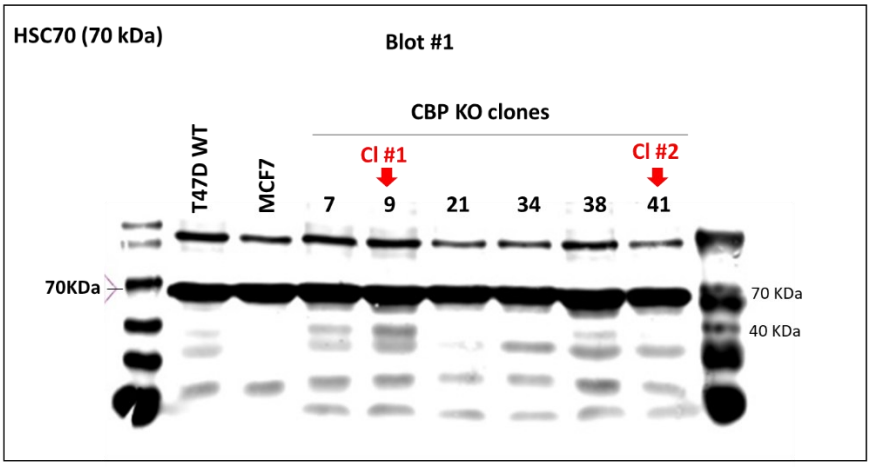

Fig. S13
(m) Raw data for Fig. S4c

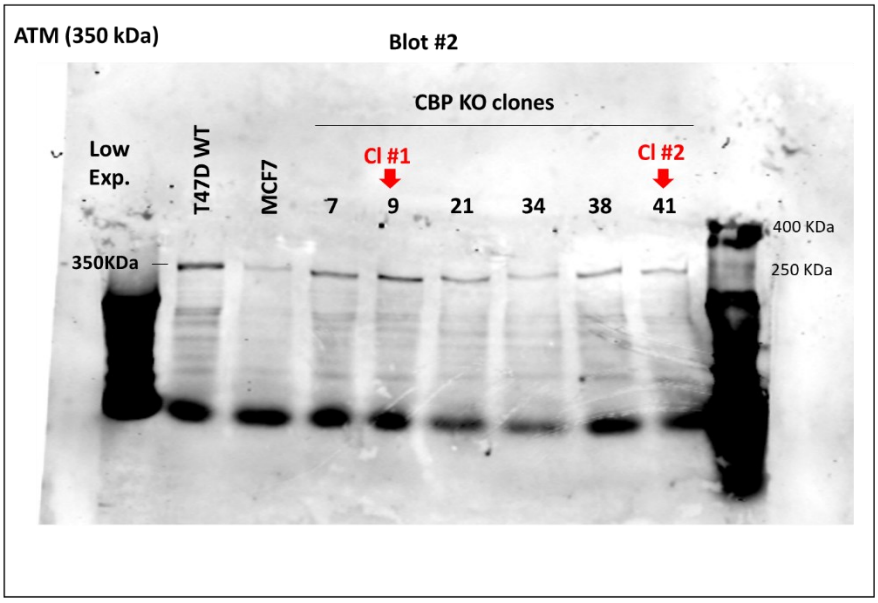

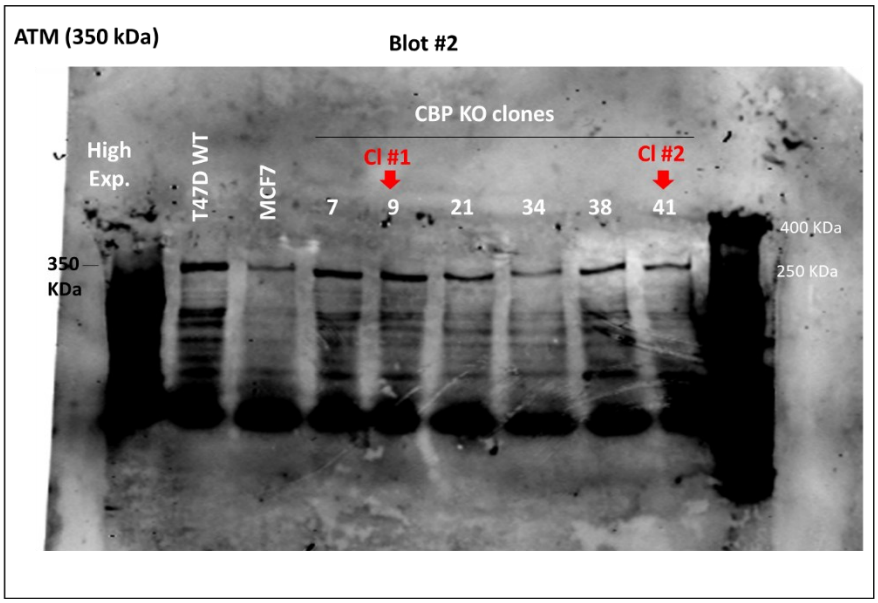

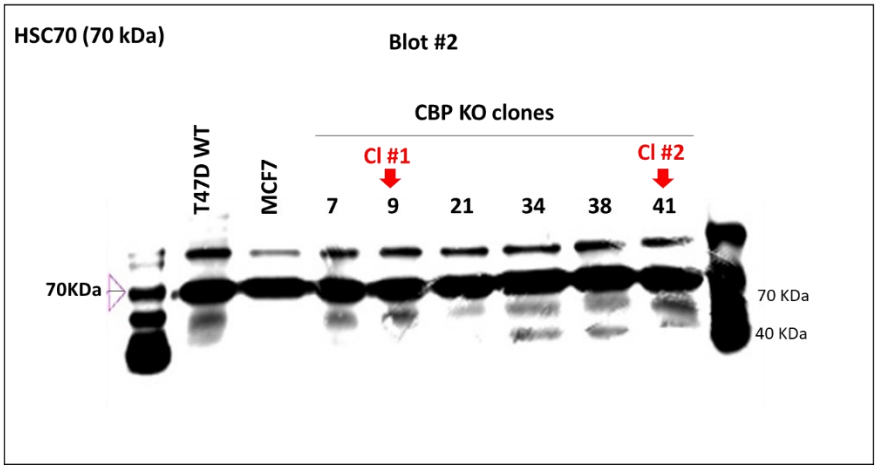

Fig. S13
(n) Raw data for Fig. S4d

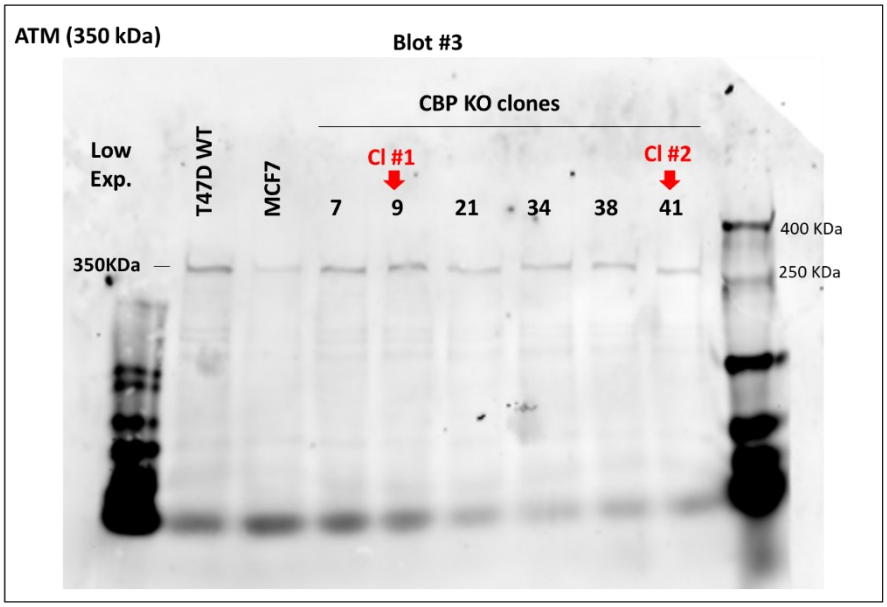

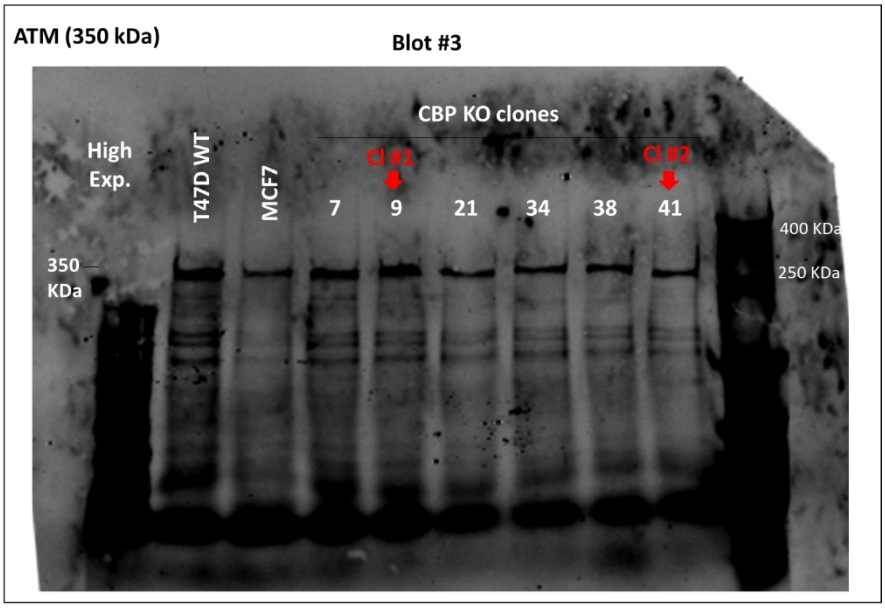

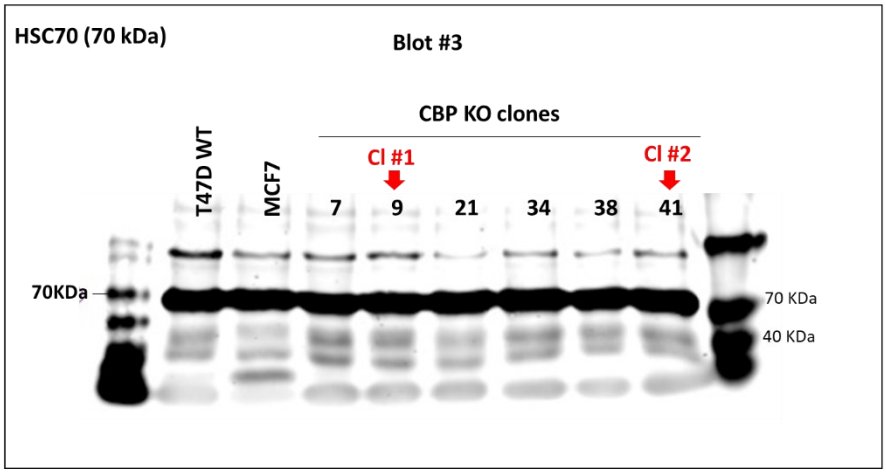

Fig. S13

(o) Raw data for Fig. S5a

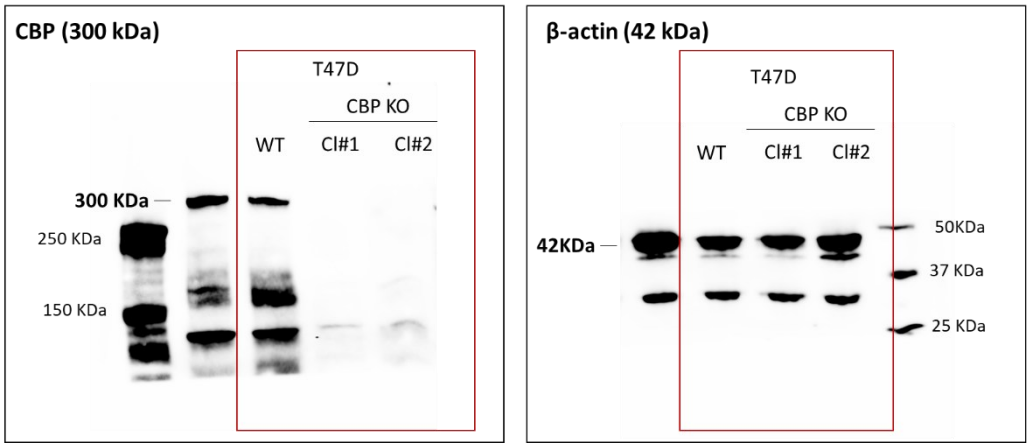

Fig. S13

(p) Raw data for Fig. S5e

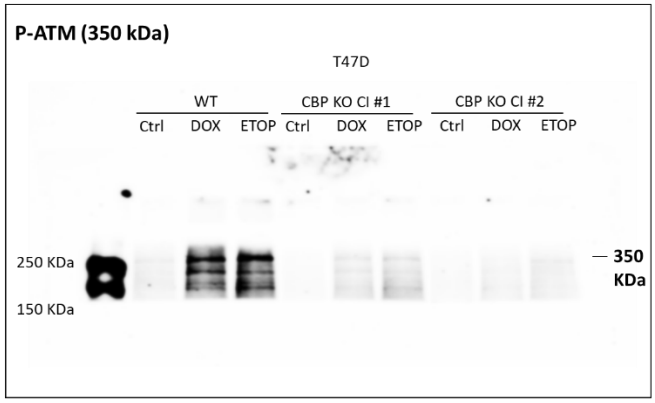

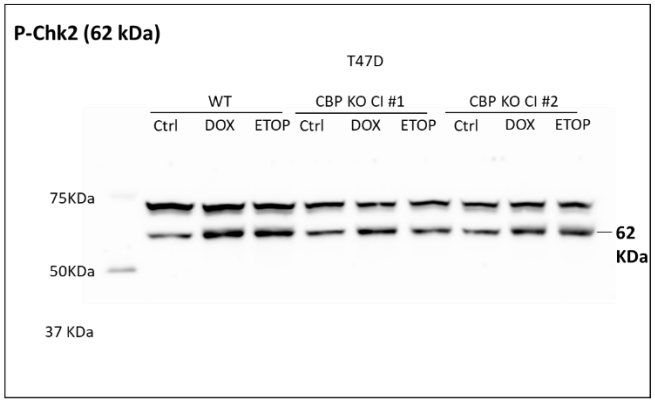

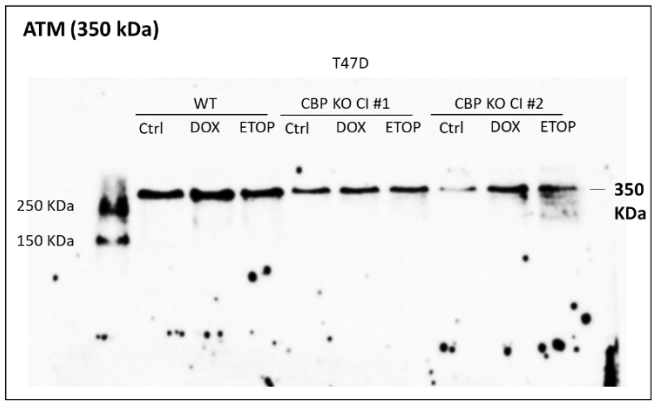

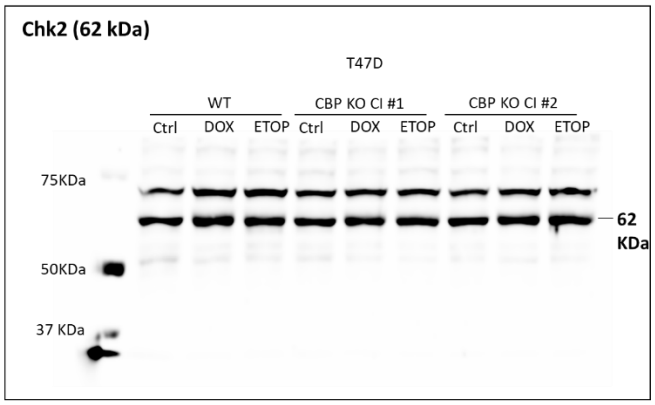

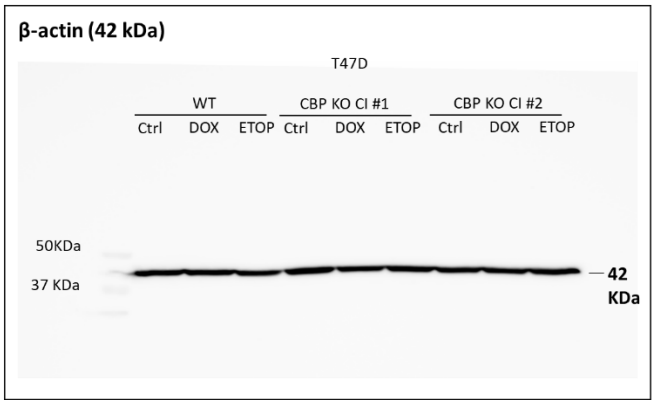

Fig. S13

(q) Raw data for Fig. S6a

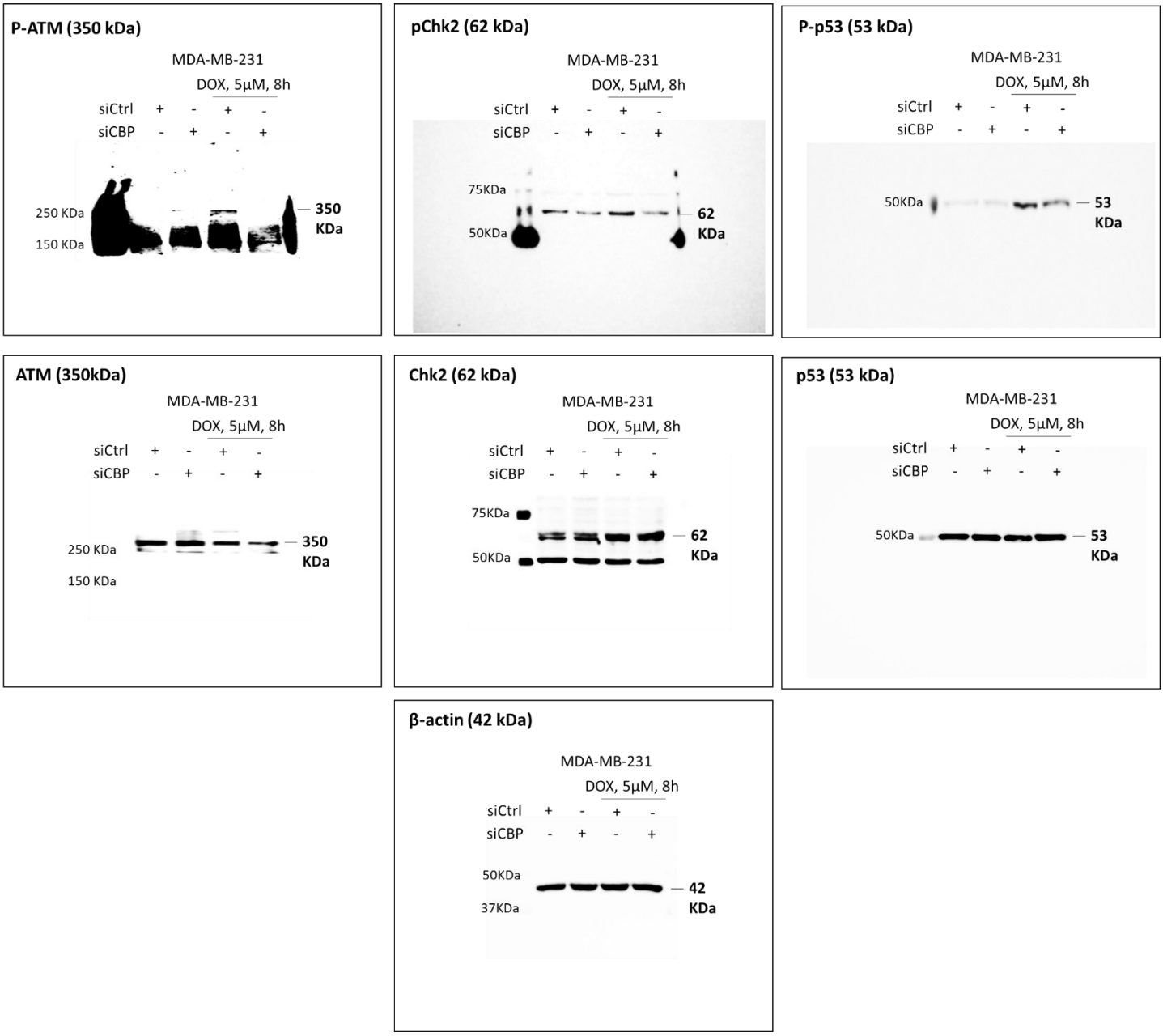

Fig. S13

(r) Raw data for Fig. S6c

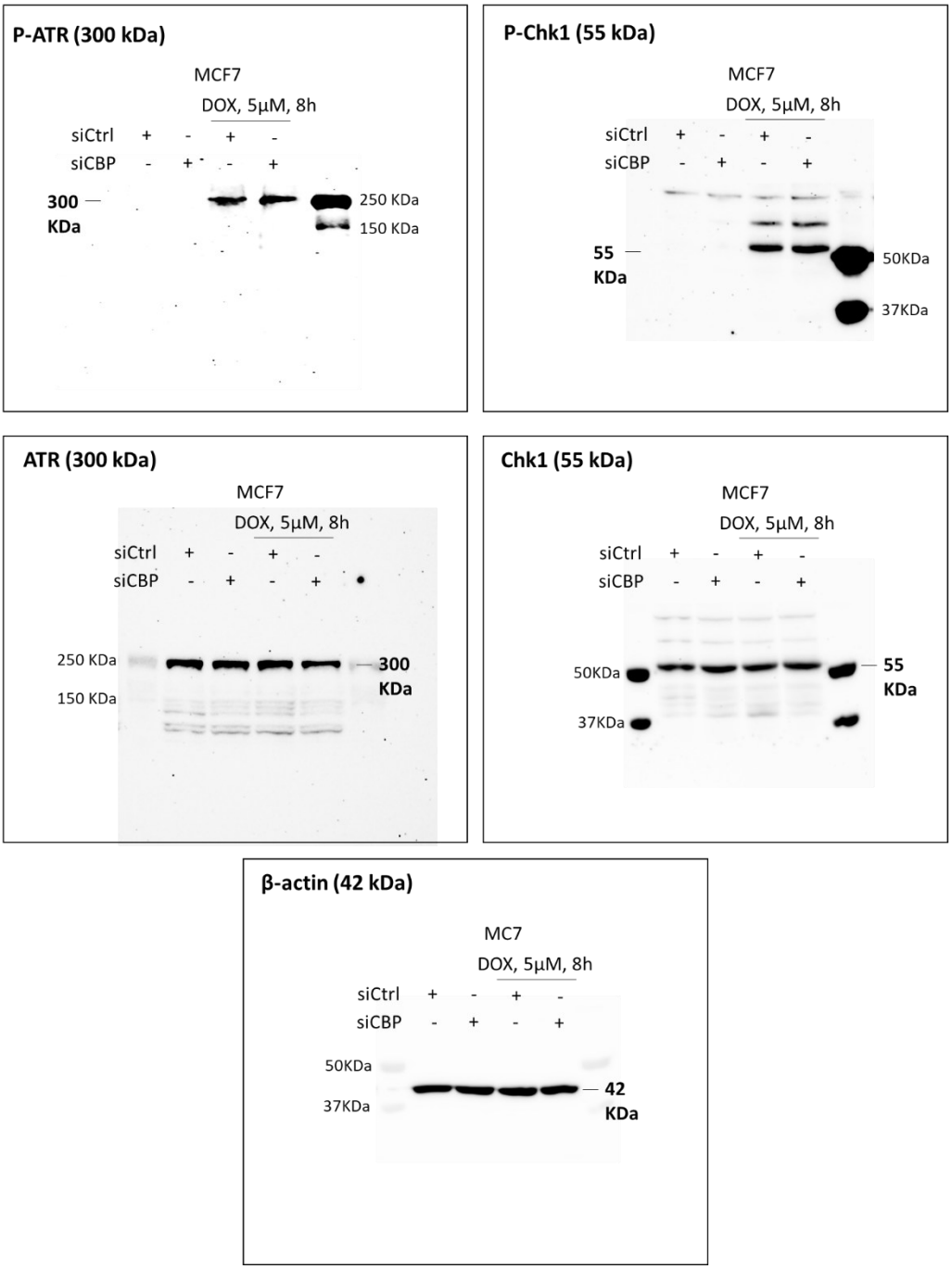

Fig. S13

(s) Raw data for Fig. S7b

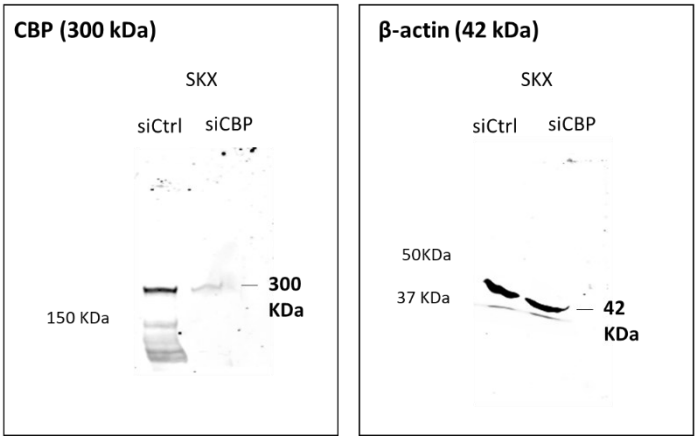

Fig. S13

(t) Raw data for Fig. S9a

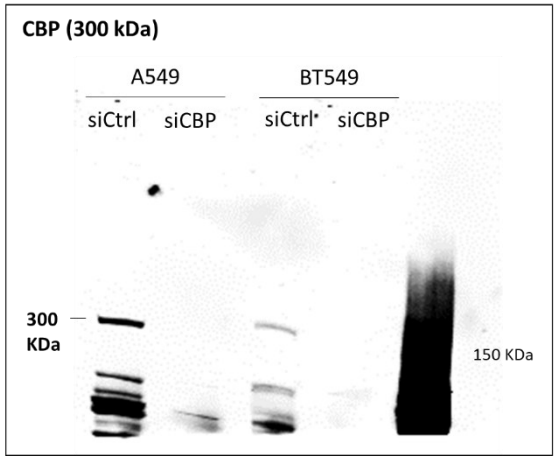

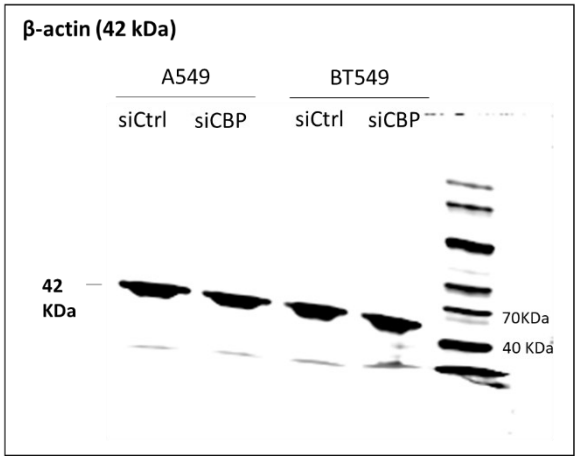

Fig. S13

(u) Raw data for Fig. S10a

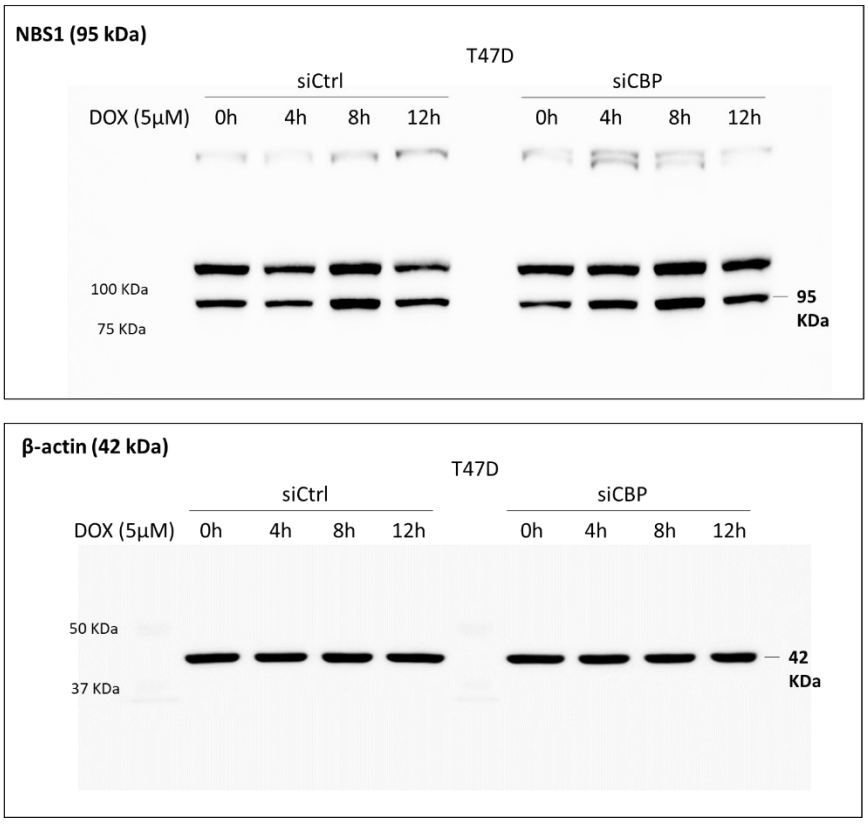

Fig. S13

(v) Raw data for Fig. S11a

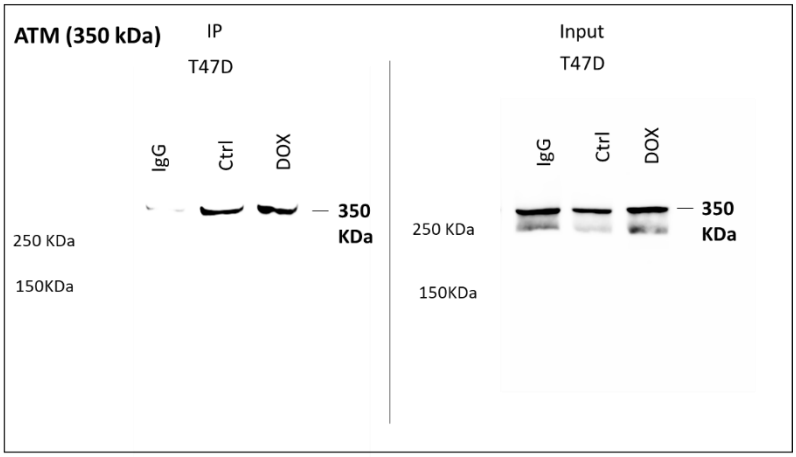

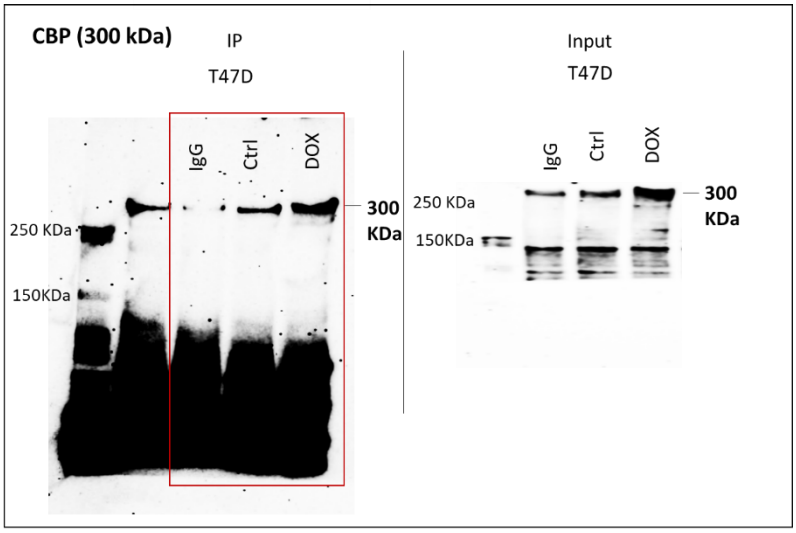

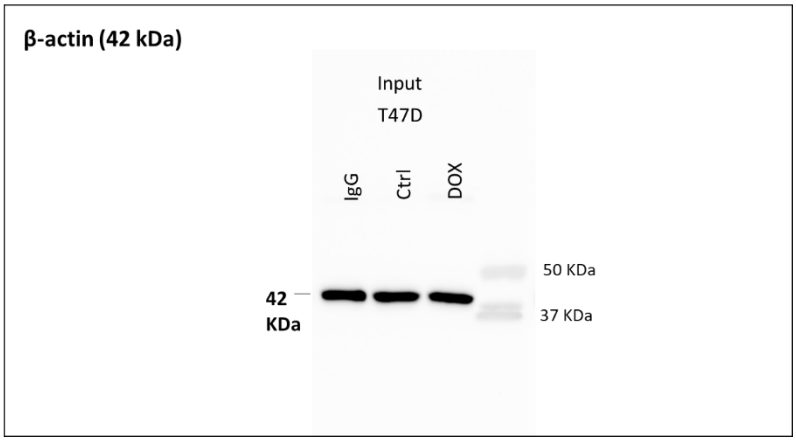

Fig. S13

(w) Raw data for Fig. S11b

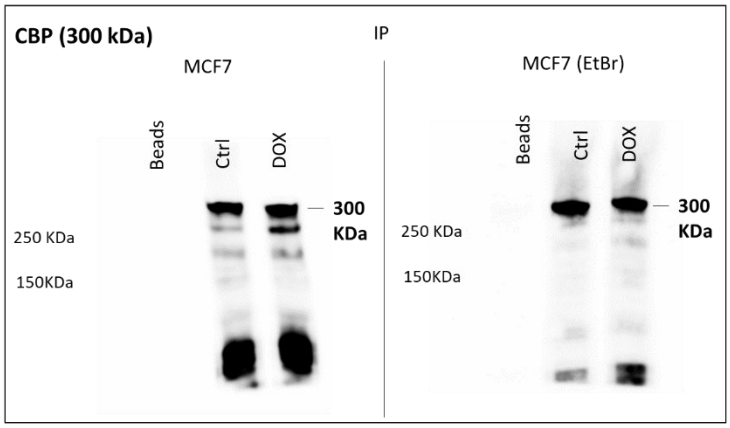

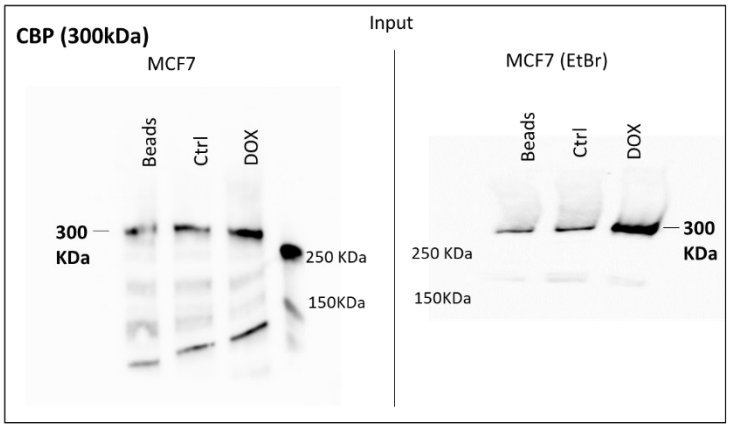

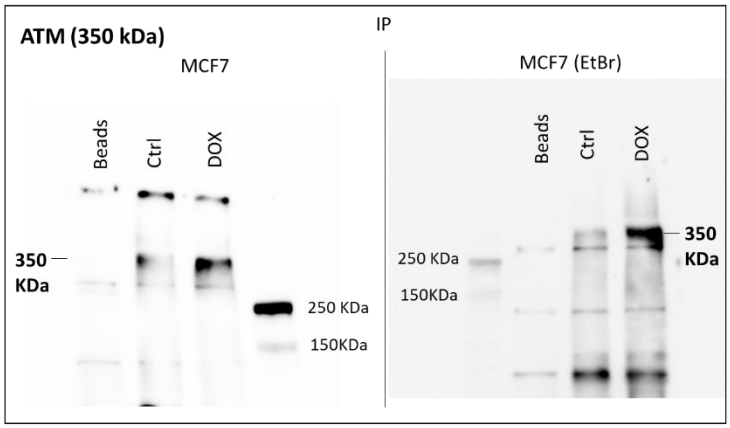

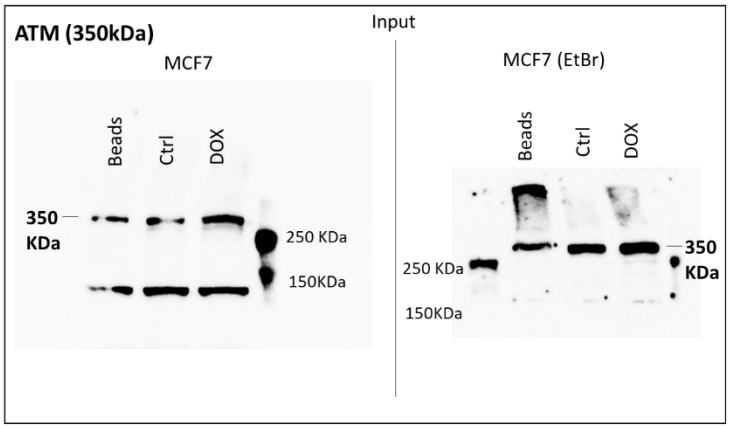

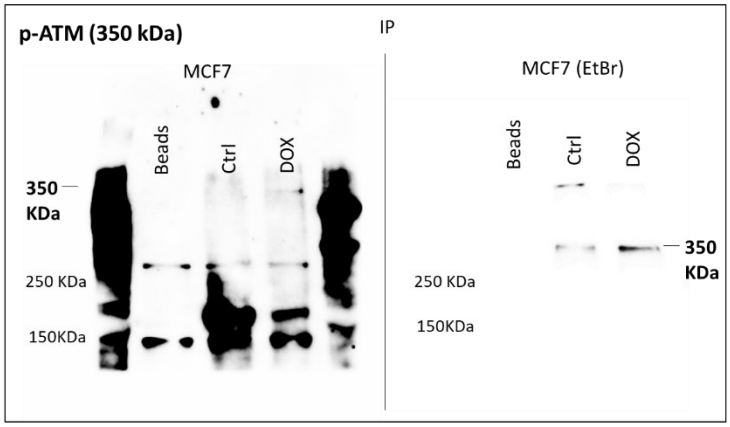

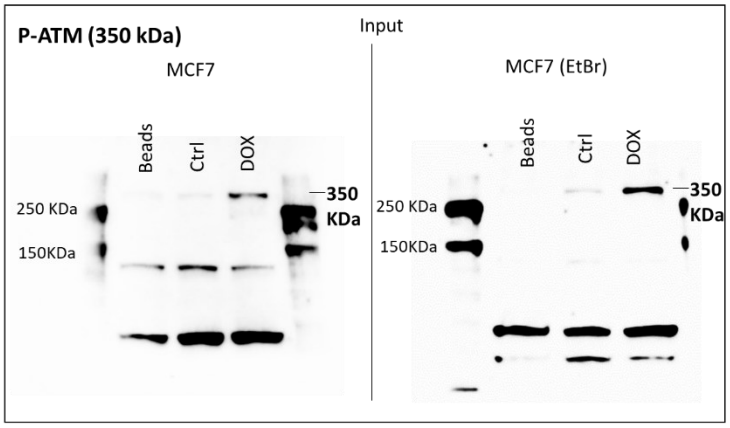

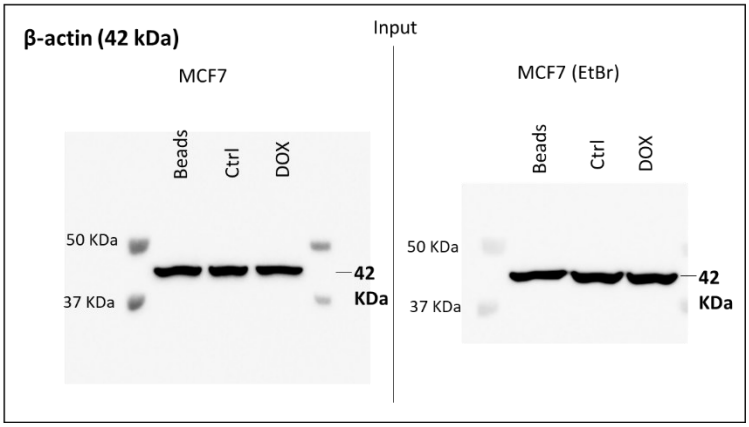

Fig. S13

(x) Raw data for Fig. S12b

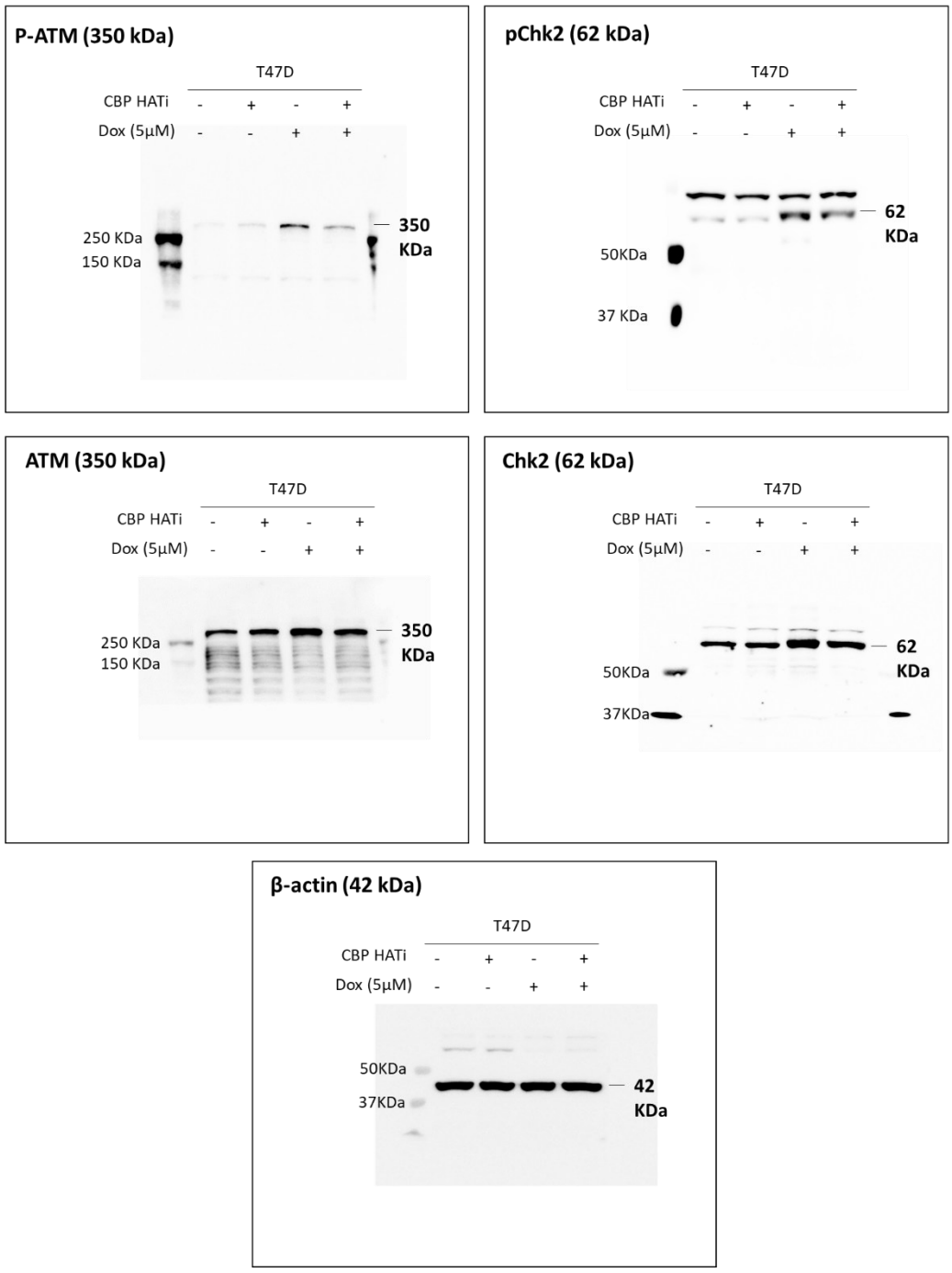

Fig. S13

(y) Raw data for Fig. S12e

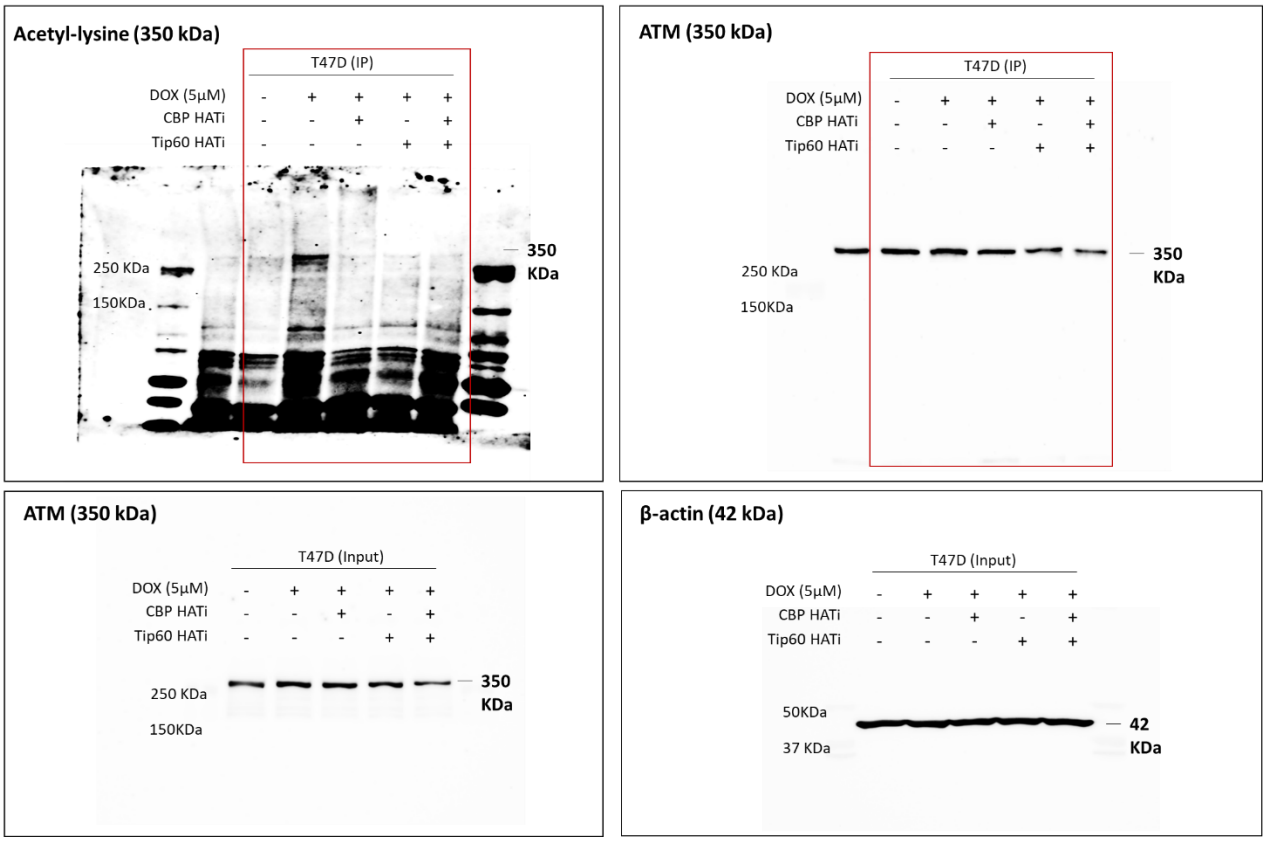

Fig. S13

(z) Raw data for Fig. S12f